Environmental Science & Technology

Article

Cite This: Environ. Sci. Technol. 2019, 53, 5272−5281

pubs.acs.org/est

Oxidation of Pharmaceuticals by Ferrate(VI) in Hydrolyzed Urine: Effects of Major Inorganic Constituents

Cong Luo,[†] Mingbao Feng,[‡] Virender K. Sharma,*[,‡] and Ching-Hua Huang*[,†]

[†]School of Civil and Environmental Engineering, Georgia Institute of Technology, Atlanta, Georgia 30332, United States

[‡]Department of Environment and Occupational Health, School of Public Health, Texas A&M University, College Station, Texas 77843, United States

Supporting Information

ABSTRACT: Destruction of pharmaceuticals excreted in urine can be an efficient approach to eliminate these environmental pollutants. However, urine contains high concentrations of chloride, ammonium, and bicarbonate, which may hinder treatment processes. This study evaluated the application of ferrate(VI) ($Fe^{VI}O_4^{2-}$, Fe(VI)) to oxidize pharmaceuticals (carbamazepine (CBZ), naproxen (NAP), trimethoprim (TMP), and sulfonamide antibiotics (SAs)) in synthetic hydrolyzed human urine and uncovered new effects from urine's major inorganic constituents. Chloride slightly decreased pharmaceuticals' removal rate by Fe(VI) due to the ionic strength effect. Ammonium (0.5 M) in undiluted hydrolyzed urine posed a strong scavenging effect, but lower concentrations (≤0.25 M) of ammonium enhanced the pharmaceuticals' degradation by 300 μM Fe(VI), likely due to the reactive ammonium complex form of Fe(V)/Fe(IV). For the first time, bicarbonate was found to significantly promote the oxidation of aniline-containing SAs by Fe(VI) and alter the reaction stoichiometry of Fe(VI) and SA from 4:1 to 3:1. In depth investigation indicated that bicarbonate not only changed the Fe(VI)/SA complexation ratio from 1:2 to 1:1 but provided a stabilizing effect for Fe(V) intermediate formed in situ, enabling its degradation of SAs. Overall, the results of this study suggested that Fe(VI) is a promising oxidant for the removal of pharmaceuticals in hydrolyzed urine.

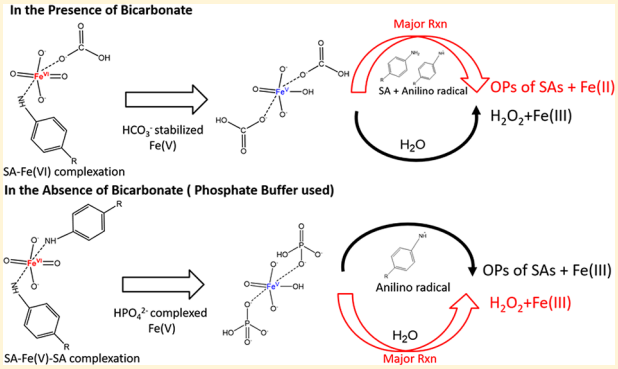

INTRODUCTION

According to the National Ambulatory Medical Care Survey in 2014,[1] the number of pharmaceuticals prescribed or provided in the U.S. was about 3.2 billion. A large portion of the pharmaceuticals are excreted unchanged or as metabolites in urine and feces and eventually are found in sewage treated at wastewater treatment plants (WWTPs). Except for highly advanced treatment processes such as reverse osmosis or advanced oxidation processes (AOPs), most WWTPs cannot effectively remove the pharmaceutical micropollutants in sewage, resulting in their release to the natural environment and posing risks to the aquatic ecosystem owing to their toxicity and potential to induce drug resistance.[2] As human urine accounts for <1% of municipal wastewater by volume but contributes a major mass load of pharmaceuticals,[3−5] degrading pharmaceuticals in urine would be an efficient way to reduce the harm of excreted pharmaceuticals to the environment.

Urine can be separately collected by urine-diverting flush toilets and waterless urinals and piped to storage tanks.[6,7] Fresh urine after excretion naturally transforms into hydrolyzed urine within hours by bacterial processes.[8] The hydrolyzed urine collected in the urine-diversion system can be a candidate for pharmaceutical removal as well as nutrient recovery. However, research to date on the removal of pharmaceuticals and their metabolites from urine has been scarce. Nanofiltration membranes,[9] strong-base anion-exchange resins,[10,11] electrodialysis,[12] and biochar[13] have been investigated to physically separate pharmaceuticals from urine but generate pharmaceutical wastes that still require treatment. Studies have investigated ozonation,[14] UV/H_2O_2, and UV/pexroxydisulfate (PDS)[15,16] for the destruction of pharmaceuticals in urine. However, the strong scavenging effects of the urine matrix, particularly from the high concentrations of chloride, ammonium, and bicarbonate, significantly decrease the pharmaceutical removal efficiency. Thus, developing a new AOP that is more resistant to the urine matrix effects for the degradation of pharmaceuticals is highly desirable.

Ferrate(VI) ($Fe^{VI}O_4^{2-}$, Fe(VI)) is considered an environmentally friendly oxidant to destruct pharmaceuticals in the hydrolyzed urine. Over the past decade, Fe(VI) has emerged as

Received: January 1, 2019
Revised: March 28, 2019
Accepted: April 1, 2019
Published: April 1, 2019

DOI: 10.1021/acs.est.9b00006
Environ. Sci. Technol. 2019, 53, 5272−5281

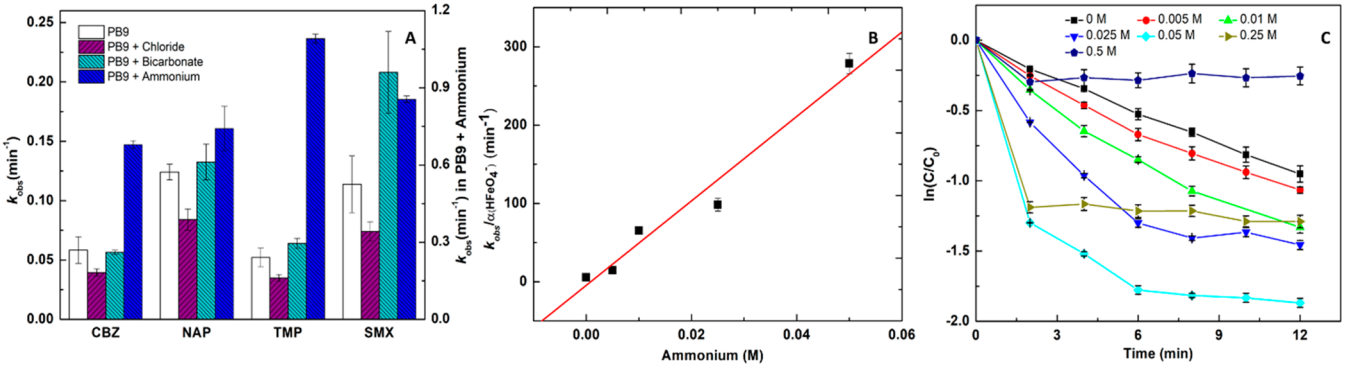

Figure 1. (A) Effect of inorganic ions on Fe(VI) oxidation of pharmaceuticals. Initially, [pharmaceutical] = 10.0 μM, [Fe(VI)] = 300.0 μM, [Cl^-] = 0.1 M, [HCO_3^-] = 0.25 M, [ammonium] = 0.01 M (n = 3 for HCO_3^- group and n = 2 for the rest of the groups). Effect of ammonium on Fe(VI) oxidation of SMX in phosphate buffer (B) and in synthetic hydrolyzed urine (C) (n = 2). Initially, [SMX] = 10.0 μM, [Fe(VI)] = 300.0 μM, [ammonium] = 0–0.5 M. All reactions were at pH 9.0 and 25.0 °C.

a novel oxidant to remove contaminants and micropollutants including pharmaceuticals.[17−26] Fe(VI) is likely less susceptible to urine matrix's scavenging effects than other common AOPs. Unlike hydroxyl radicals ($^{\bullet}OH$) and sulfate radicals ($SO_4^{\bullet-}$), Fe(VI) reacts much more slowly with NH_3 at pH 9.0–9.3 (rate constants of NH_3 with Fe(VI), $^{\bullet}OH$, and $SO_4^{\bullet-}$ are 1.2 × 10^{-1}, 1.0 × 10^8, and 1.4 × 10^7 $M^{-1}{\cdot}s^{-1}$, respectively),[27−29] and has negligible reactivity on HCO_3^-/CO_3^{2-} and Cl^-.[30] Furthermore, the natural pH (~9.0) of hydrolyzed urine is optimal for Fe(VI) oxidation processes due to excellent stability and easy handling of Fe(VI) at this alkaline pH,[31,32] and thus, no sample pH adjustment is needed to promote Fe(VI) reaction.

Therefore, the objective of this study was to assess the efficacy of Fe(VI) to degrade pharmaceuticals in hydrolyzed urine matrix. Several pharmaceuticals (carbamazepine (CBZ), naproxen (NAP), trimethoprim (TMP), and various sulfonamide antibiotics (SAs) including sulfamethoxazole (SMX)) that are frequently detected in the environment[33−35] were selected as the representative contaminants. Experiments were conducted using synthetic hydrolyzed urine (SHU)[36,37] with modifications or buffered solutions to delineate the specific effects of chloride, ammonia, and bicarbonate. As will be discussed later, enhanced reaction rates of pharmaceutical degradation in simulated urine and buffer solution matrices by Fe(VI) were observed by ammonia and bicarbonate. To the best of our knowledge, the finding of the bicarbonate enhancement effect during Fe(VI) oxidation is among the first. Additional experiments including stoichiometry determination between Fe(VI) and 2,2′-azino-bis(3-ethylbenzothiazoline-6-sulfonate) (ABTS) were conducted to obtain mechanistic insight on the enhanced effect of bicarbonate.

MATERIALS AND METHODS

Chemicals. Sources of chemicals and reagents are provided in the Supporting Information (SI) Text S1. Structures and chemical properties of the target pharmaceuticals are shown in Table S1.

Reaction Matrices. SHU was prepared following the literature recipe[15] as described in Table S2. SHU contained 0.5 M total ammonia (NH_3 + NH_4^+), 0.25 M total carbonate (HCO_3^- + CO_3^{2-}), 0.1 M chloride, 7.40 mM creatinine, 1.28 mM creatine, 0.17 mM hippuric acid, as well as Na^+, K^+, SO_4^{2-}, and phosphate. The SHU pH was adjusted to 9.0 using concentrated solutions of NaOH and NaH_2PO_4. For comparison, SHU without ammonium was also prepared by removing NH_4OH addition and adding additional 250 mM $NaHCO_3$ to substitute NH_4HCO_3 in the recipe. To evaluate the effect of individual urine constituents, phosphate buffer (10.0 mM) solution at pH 9.0 (PB9) was spiked with specific urine constituents at various concentrations and compared with the PB9 control matrix without urine constituents. At pH 9.0, ammonium (NH_4^+) and bicarbonate (HCO_3^-) are the dominant species in concentration. However, in the subsequent discussion, ammonium and bicarbonate referred to the total ammonia and total carbonate, respectively, without excluding the minor species.

Oxidation Experiments and Analysis. PB9, modified PB9, or SHU solutions (50.0 mL) were first spiked with the target pharmaceutical (10.0 μM). Then, 2.97 mg of potassium ferrate(VI) solid was weighed and added immediately to the reaction solution (achieving 300.0 μM) to initiate the oxidation process. Sample aliquots were taken from the reaction solution at predetermined time intervals and quenched immediately by sodium thiosulfate (2.5 mM).[38] The pH was checked before and after the reaction by a pH meter, and the change was never larger than 0.2 pH unit. The degradation of pharmaceuticals was monitored by high-performance liquid chromatography (HPLC)–diode-array detection (DAD), and the transformation products of SMX by Fe(VI) were analyzed using solid-phase extraction (SPE) followed by HPLC–high-resolution mass spectrometry (LC–HRMS) analysis. Detailed analytical methods are described in Text S2. Experiments to study the reaction stoichiometry of Fe(VI) and SMX (or ABTS) are described in Text S3. 1,10-Phenanthroline was used to confirm the final oxidation state of iron after Fe(VI) oxidation of SMX, and the method followed a previous study.[39]

Complexation of Fe(VI) and SAs. The complexation between Fe(VI) and SAs was studied using UV–vis spectrophotometry. Different SAs at concentrations 25.0–800.0 μM were added into 8.0 mL of PB9 and modified PB9 solutions with either 0.05 or 0.25 M bicarbonate, respectively. Two milliliters of 500.0 μM freshly prepared Fe(VI) stock solution (in 10.0 mM PB9) was added to initiate the complexation. Within 15 s, sample aliquot was taken and transferred into a quartz cell and analyzed by a UV–vis spectrophotometer (Agilent 8453) at 190 to 1200 nm.

DOI: 10.1021/acs.est.9b00006
Environ. Sci. Technol. 2019, 53, 5272–5281

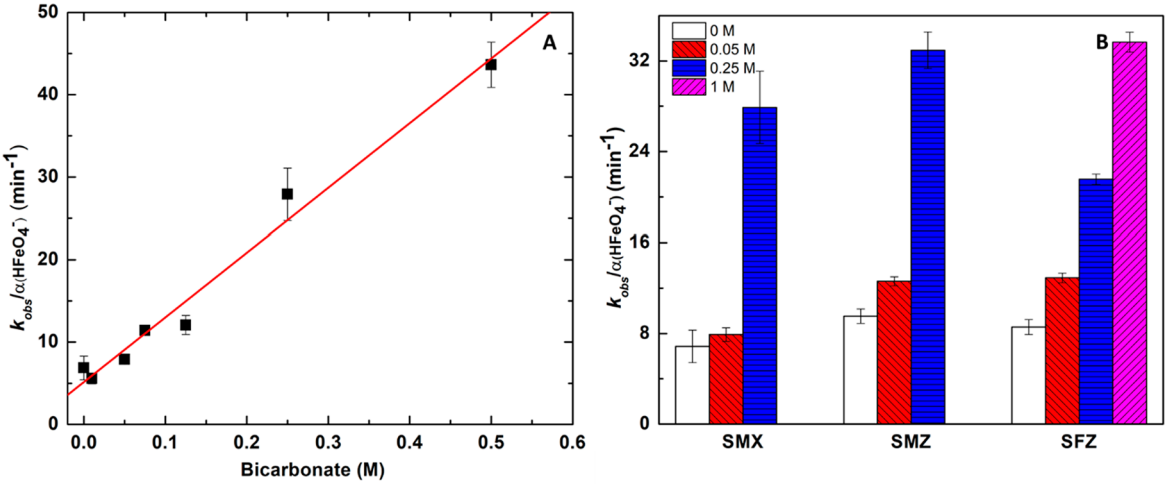

Figure 2. (A) Effect of bicarbonate concentration on Fe(VI) oxidation of SMX; n = 3. (B) Effect of bicarbonate on Fe(VI) oxidation of different SAs. Initially, [SA] = 10.0 μM, [Fe(VI)] = 300.0 μM, [HCO_3^-] = 0−1.0 M, pH = 9.0, T = 25.0 °C, n = 2 for SMZ and SFZ, and n = 3 for SMX. R^2 = 0.989−0.995 for the rate constants.

RESULTS AND DISCUSSION

Impacts of Urine Constituents on Pharmaceutical Degradation by Fe(VI). The removal (based on loss of parent compounds) of four pharmaceuticals in SHU using a low dose of Fe(VI) (300.0 μM or 0.06 g(K_2FeO_4)·L^{-1}) ranged from 20% to 35% within 1 min (Figure S1) due to the strong scavenging effects from some of the urine constituents. Ammonium was found to be a major scavenger due to its exceedingly high concentration in urine (N_T = 0.5 M) despite of a low rate constant with Fe(VI) (k = 0.119 $M^{-1}\cdot s^{-1}$).[28] The scavenging effect of ammonium was confirmed by separate experiments in which 300.0 μM Fe(VI) was rapidly consumed by 0.5 M ammonium in PB9, leading to negligible removal of pharmaceuticals. To overcome this inhibitory effect, Fe(VI) dosage was increased to 900.0 μM, and 86% removal of SMX in SHU was achieved (Figure S1).

When the Fe(VI) oxidation was conducted in comparable, but NH_3-free, SHU, significant degradation of pharmaceuticals occurred, and the associated pseudo-first-order rate constants (k_{obs} in min^{-1}) were obtained (Figure S2). Specifically for CBZ, NAP, and TMP, the scavenging effect of the NH_3-free urine matrix was obvious: the oxidation rate constants of pharmaceuticals by Fe(VI) were approximately half of those in the PB9 matrix. Surprisingly, the degradation rate of SMX by Fe(VI) in the NH_3-free SHU was only slightly lower than that in the PB9 matrix, indicating the possible structure-specific enhancement effects from urine components. In the following discussion, k_{obs} (in min^{-1}) was used to compare the impacts of inorganic urine constituents when they were present or absent in the reactions.

Chloride. Compared to PB9, chloride (0.1 M) in PB9 slightly inhibited the oxidation rate of pharmaceuticals by Fe(VI) (Figure 1A), compared to the strong scavenging effect of chloride on $SO_4^{\bullet-}$-based AOPs.[15,16] Previous studies reported that the dissociation constants of Fe(VI) ($H_3FeO_4^+$) as pK_1 = 1.6, pK_2 = 3.5, and pK_3 = 7.3. The value of pK_3 for the monoprotonated Fe(VI) species, $HFeO_4^-$, decreased with increasing ionic strength according to the eq 1[40]

$$pK_3 = 4.247 + \frac{888.5}{T} + 0.8058I^{0.5} + 0.5144I - \frac{529.43I^{0.5}}{T} \quad (1)$$

where I = ionic strength and T = absolute temperature.

Additionally, $HFeO_4^-$ was the major reactive species in the oxidation of SMX by Fe(VI) at pH 6.93−9.50.[41] A lower pK_3 value would lead to a decreased fraction of $HFeO_4^-$ at pH 9.0 and thus slower reaction. By dividing the k_{obs} by the corresponding fraction of the $HFeO_4^-$ species, the obtained empirical rate constants (i.e., $k_{obs}/\alpha(HFeO_4^-)$) showed less than 10% of difference with or without Cl^- for all four pharmaceuticals (see Table S3). These results suggested that the mild inhibitory effect of chloride was presumably due to the ionic strength that influenced the acid dissociation constants of Fe(VI).

Ammonium. Compared to PB9, ammonium (0.01 M) in PB9 resulted in 7−20 times increase in k_{obs} for the oxidation of four pharmaceuticals by Fe(VI) (Figure 1A and Figure S3). Moreover, when ammonium was added at different concentrations (0−0.05 M), the obtained empirical rate constants ($k_{obs}/\alpha(HFeO_4^-)$ according to different ionic strengths under different ammonium concentrations) increased linearly with ammonium concentration for the oxidation of SMX by Fe(VI) (Figure 1B). The relationship in Figure 1B is the impact of ammonium after correcting the ionic strength effect, indicating a truly enhanced effect of ammonium on the oxidation of SMX by Fe(VI). A similar phenomenon was recently found in the oxidation of flumequine by Fe(VI) in the presence of 0.5−10.0 mM ammonium.[42] In that study, the authors proposed that ammonium conjugated with Fe(V)/Fe(IV) intermediates to form more reactive ammonium complexes of Fe(V)/Fe(IV), which could enhance the oxidation rate of flumequine by 5−12 times. High-valent iron complexes containing nitrogen ligands tend to have high reactivity with substrates.[43,44] Note that the negative impact of ammonium on several advanced oxidation processes (AOPs) is well-known and has been seen in the treatment of urine using ozone,[14] UV/H_2O_2, and UV/PDS.[15,16] Indeed, as shown in Figure 1C, a very high concentration of ammonium (e.g., 0.5 M in SHU) posed a strong scavenging effect on Fe(VI) oxidation. However, unlike other AOPs, enhanced removal of pharmaceuticals by 300 μM

DOI: 10.1021/acs.est.9b00006
Environ. Sci. Technol. 2019, 53, 5272−5281

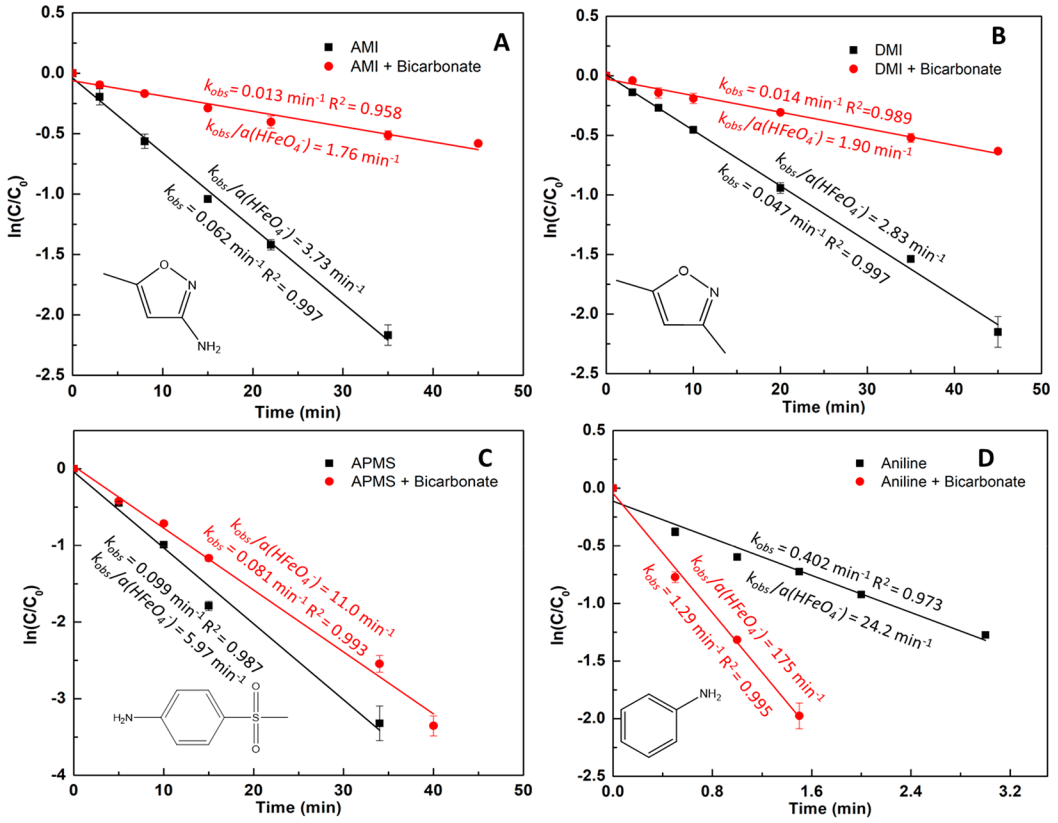

Figure 3. Degradation of AMI (A), DMI (B), APMS (C), and aniline (D) by Fe(VI) with and without bicarbonate. Initially, [substrate] = 10.0 μM, [Fe(VI)] = 300.0 μM, [HCO_3^-] = 0.25 M, pH = 9.0, T = 25.0 °C, and n = 2.

Fe(VI) was observed when the ammonium concentration was equal to or lower than 0.25 M (i.e., [Fe(VI)]/[ammonium] ≥ 0.0012). Considering that source-separated urine collected from the NoMix toilets and urinals is usually diluted to some extent,[7] the ammonium concentration in such collected urine is expected to be lower than the ammonium concentration (0.5 M) used in the SHU recipe, which simulated the human urine without any dilution. Moreover, if the real urine is subjected to pretreatment processeses (e.g., air-stripping) to recover N-nutrients prior to the treatment for pharmaceuticals, the ammonium concentration is expected to be much lower. Thus, the enhanced effect of ammonium on the oxidation of pharmaceuticals by Fe(VI) can prevail in such real urine matrix with a lower ammonium concentration.

Bicarbonate. Compared to PB9, bicarbonate (0.25 M) in PB9 had little effect on the Fe(VI) oxidation of CBZ, NAP, and TMP but significantly increased the degradation rate of SMX by Fe(VI) (Figure 1A). This enhanced effect is a significant contrast to the strong scavenging effect of bicarbonate on $^{\bullet}$OH-based AOPs[15,16] and has not been reported in the literature. Further experiments were conducted with different concentrations of bicarbonate and the empirical rate constants ($k_{obs}/\alpha(HFeO_4^-)$) were obtained. As shown in Figure 2A, a strong linear correlation between the empirical rate constant ($k_{obs}/\alpha(HFeO_4^-)$) of SMX oxidation by Fe(VI) and bicarbonate concentration was observed, indicating a truly enhanced effect of bicarbonate without the ionic strength influence. The bicarbonate enhancement effect was observed not only for SMX but also in the oxidation of other SAs (sulfamethazine (SMZ) and sulfamethizole (SFZ)) by Fe(VI). As Figure 2B shows, the empirical rate constants of Fe(VI) oxidation of SMX and SMZ increased by 2.5−4.1 folds in the presence of 0.25 M bicarbonate compared to those without bicarbonate, whereas a similar magnitude of rate enhancement for the Fe(VI) oxidation of SFZ required a higher bicarbonate concentration of 1.0 M.

Elucidating the Bicarbonate Enhancement Effect. The new discovery that bicarbonate can enhance the Fe(VI) oxidation of SAs compared to that in the absence of bicarbonate suggests that bicarbonate may induce a new reaction mechanism, which requires further investigation. Previous work by Chen and Hoffman found that sulfur-containing compounds can react rapidly with $CO_3^{\bullet-}$,[45] which may explain the bicarbonate enhancement effect on the Fe(VI) oxidation of SAs. However, electron paramagnetic resonance (EPR) study was conducted using DMPO (Text S2), and the results excluded the generation of $CO_3^{\bullet-}$ in the Fe(VI) + bicarbonate system (Figure S4). Therefore, the mechanism of bicarbonate enhancement effect required elucidation. In this study, SMX was chosen as the main model compound to further probe the bicarbonate enhancement effect.

Reaction Stoichiometry. Experiments showed that the oxidation of SMX by Fe(VI) in the presence of bicarbonate exhibited different reaction stoichiometry compared to that in the absence of bicarbonate. A previous study[46] reported that the oxidation of SMX by Fe(VI) followed a stoichiometry of 4:1 for [Fe(VI)]/[SMX], which led to the evolution of one mole of oxygen per mole of SMX accompanying reduction of Fe(VI) to Fe(III) (eq 2). However, a reaction stoichiometry of 3:1 for [Fe(VI)]/[SMX] was observed in the presence of 0.25 M bicarbonate (Figure S5A), and Fe(II) was identified as the likely end product of Fe(VI) reduction based on Fe(II)−

DOI: 10.1021/acs.est.9b00006
Environ. Sci. Technol. 2019, 53, 5272−5281

Scheme 1. Proposed Reaction Pathways of Fe(VI) Oxidation of SMX in the Absence/Presence of Bicarbonate[a]

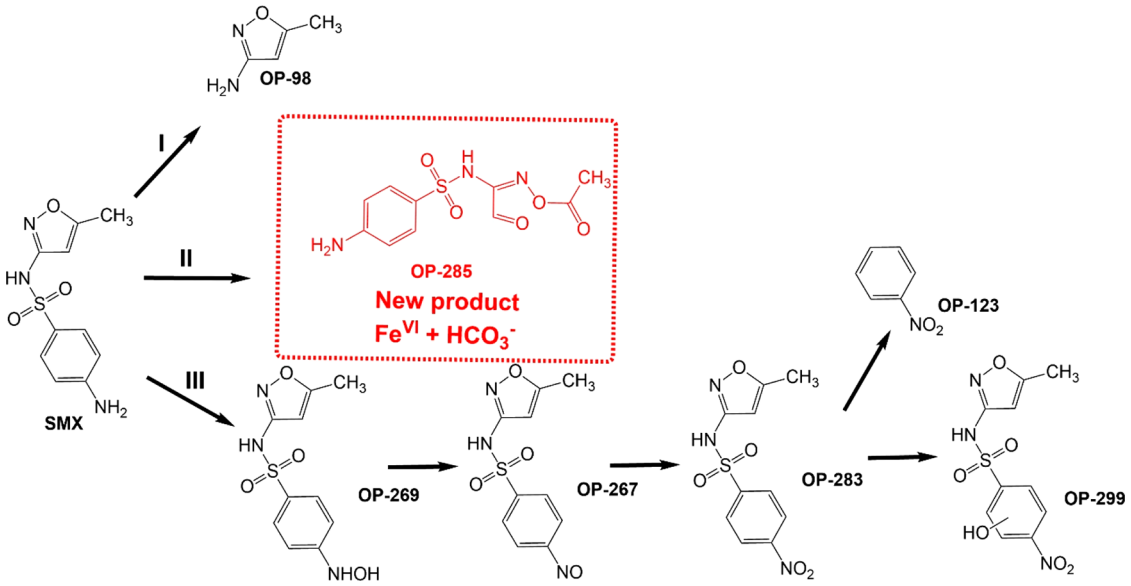

[a]Initially, [SMX] = 10.0 μM, [Fe(VI)] = 300.0 μM, [HCO_3^-] = 0 or 0.25 M, pH = 9.0, and T = 25.0 °C.

phenanthroline complex observed at 510 nm (Figure S5B). This reaction is shown in eq 3.

$$4Fe(VI) + SMX \rightarrow 4Fe(III) + O_2 + products \quad (2)$$

$$3Fe(VI) + SMX + bicarbonate \rightarrow 3Fe(II) + products \quad (3)$$

On the basis that the reaction stoichiometry was changed in the presence of bicarbonate, it strongly suggested that the presence of bicarbonate affected the electron transfer processes of Fe(VI), likely involving different Fe intermediates and leading to different end products of Fe(VI) (i.e., Fe(III) vs Fe(II), respectively). Additionally, the lower reaction stoichiometry in the presence of bicarbonate is a favorable finding, because it indicates a lower Fe(VI) demand and higher reaction efficiency in degrading the same amount of SMX.

Reactive Moiety of SMX. To determine the initial attack of Fe(VI) on SMX, reactions of substructure compounds (3-amino-5-methylisoxazole (AMI), 3,5-dimethylisoxazole (DMI), 4-aminophenyl methyl sulfone (APMS), and aniline) with Fe(VI) were examined in the presence and absence of bicarbonate at pH 9.0. As Figure 3 shows, when bicarbonate was absent, AMI and DMI were much less reactive to Fe(VI) (k_{obs} = 6.2 × 10^{-2} and 4.7 × 10^{-2} min^{-1}) than APMS and aniline (k_{obs} = 9.9 × 10^{-2} and 4.0 × 10^{-1} min^{-1}), which suggested SMX's aniline moiety (rather than the isoxazole ring moiety) with higher susceptibility to be attacked by Fe(VI). When comparing the Fe(VI) only vs Fe(VI) + bicarbonate systems, the smaller empirical rate constants were observed in AMI and DMI, whereas larger empirical rate constants were observed in aniline and APMS (containing aniline moiety) in the presence of bicarbonate. This result further indicated that the aniline moiety of SMX is most likely involved in the oxidation by Fe(VI) with the presence of bicarbonate. It also confirmed that the aniline moiety is the crucial site so that the similar bicarbonate enhancement effect was observed in Fe(VI) oxidation of other SAs. In other words, bicarbonate enhancing the oxidation reaction of Fe(VI) can be expected for other compounds that carry the aniline moiety.

Oxidation Products (OPs) of SMX in Fe(VI) Only and Fe(VI) + Bicarbonate Systems. The OPs of SMX in Fe(VI) only and Fe(VI) + bicarbonate systems at pH 9.0 were analyzed by LC−HRMS. Structural assignments of each OP were performed by product ion scans based on its MS/MS spectrum and the proposed fragments. A total of seven OPs of SMX were identified and named as OP-98, OP-123, OP-267, OP-269, OP-283, OP-285, and OP-299 according to molecular weight. MS/MS spectra and possible structures of fragments of SMX and its OPs and the evolution of their peak areas are presented in Figures S6−S8. Even though OP-98, OP-123, and OP-285's MS/MS spectra were not available, the products' evolution profiles in Figures S6 and S7 indicated high abundance of these three products during the reaction and their distribution growth over reaction time. The molecular compositions of these OPs were suggested by good mass error (<3 ppm) between the experimental and theoretical m/z values, shown in Table S4. For the fragment analysis, SMX with an m/z value of 254.05936 and retention time of 4.510 min has four major product ions at m/z 156.01144, 99.05586, 108.04486, and 92.05013, which are proposed to correspond to the cleavage of S−N bond with the generation of two former fragments, loss of SO (48 Da from m/z 156.01144), and subsequent loss of O (16 Da from m/z 108.04486), respectively (Figure S8a). As a representative product, OP-269 with a protonated species at m/z 270.05740 and chromatographic retention time at 4.397 min was proposed to be hydroxylation of aniline group in SMX molecule. This structure was tentatively confirmed by four major product ions at m/z 172.00618, 99.05589, 124.03966, and 108.04493. These MS/MS fragments were formed via similar patterns with SMX.

The proposed degradation pathways of SMX in Fe(VI) only and Fe(VI) + bicarbonate systems are shown in Scheme 1. Both systems shared similar pathways I and III. In pathway I, cleavage of the S−N bond generated OP-98 (AMI), which was also observed in other SMX oxidation systems using chlorine,[47] ozone, and permanganate.[48] In pathway III, the initial attack on the aniline group of SMX produced hydroxylamine product

DOI: 10.1021/acs.est.9b00006
Environ. Sci. Technol. 2019, 53, 5272−5281

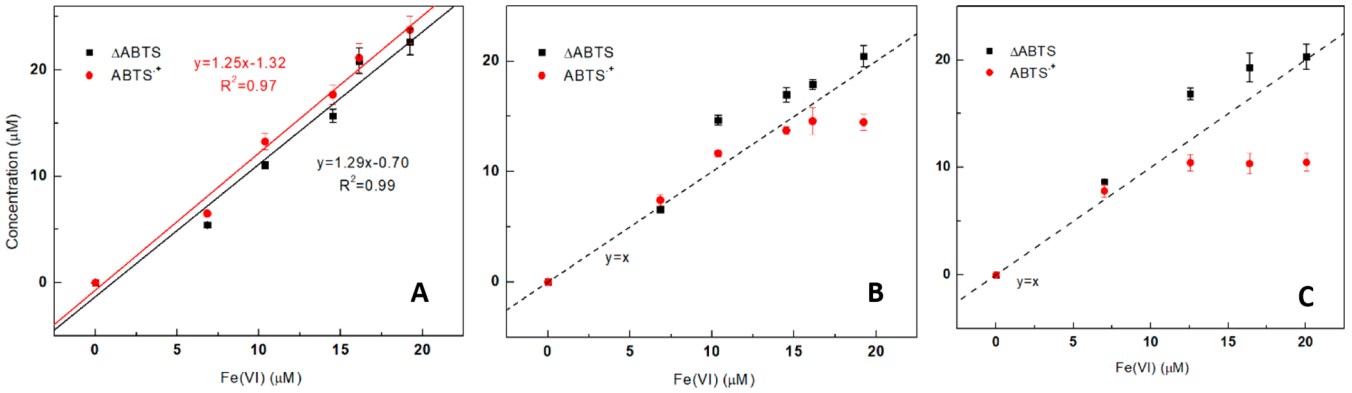

Figure 4. Reaction stoichiometries between Fe(VI), ABTS and $ABTS^{\bullet+}$ in different bicarbonate solutions. Initially, $[ABTS]_0$ = 100.0 μM, $[Fe(VI)]_0$= 0−20.0 μM, pH = 9.0, T = 25.0 °C, n = 2 and buffer conditions: (A) 10.0 mM; (B) 100.0 mM; (C) 250.0 mM bicarbonate buffer.

(OP-269) via a single-electron-transfer mechanism.[49] Later, this resulting hydroxylamine group will further collapse to nitroso group (OP-267), which can be further oxidized into nitro group (OP-283). Afterward, OP-283 can be hydrolyzed in the benzene ring part with OP-299 generated, all of which are consistent with the previous study.[46] The similar products found in Fe(VI) only system and Fe(VI)+bicarbonate system were also confirmed in acid[50]- and sulfite[51]-activated Fe(VI) systems, suggesting these generated iron intermediates (Fe(V) or Fe(IV)) could not change the OP species but alter the oxidation rate due to superior oxidation ability of Fe(V)[52,53] or Fe(IV).[54]

However, OP-123 (nitrobenzene) was found to be a new product in both systems, indicating Fe(VI)'s ability to break the S−C bond during the reaction. Pathway II only observed in the Fe(VI) + bicarbonate system suggested bicarbonate-complexed Fe(VI) can initiate the ring-opening reaction in the isoxazole moiety in SMX by attacking the C═C double bond via hydroxylation, which was also observed in the oxidation of flumequine by ammonia-complexed high-valent iron species (Fe(V) or Fe(IV)).[42]

Fe(VI) Oxidation of ABTS in the Presence of Bicarbonate. Colorless ABTS can be oxidized via the one-electron transfer mechanism to yield $ABTS^{\bullet+}$, a stable radical with intense green color. Therefore, ABTS has been widely used for quantification of different types of oxidants, such as percarboxylic acid,[55] bromine, chlorine,[56] and Fe(VI),[57] owing to its rapid reaction and simple spectrophotometric measurement with high sensitivity. In the reaction between Fe(VI) and ABTS, a stoichiometry of 1:1 between Fe(VI) loss and $ABTS^{\bullet+}$ generation was determined, and Fe(V) was proposed as the major iron intermediate species.[57,58] The produced Fe(V) undergoes subsequent self-decay in phosphate buffer solution since the stoichiometry between Fe(VI) and ABTS consumption was also found to be 1:1,[57,59] indicating phosphate-complexed Fe(V) favors its reaction toward H_2O (self-decay) instead of ABTS.[59]

Herein, ABTS was chosen as a model compound to investigate the bicarbonate effect on Fe(VI) oxidation, especially when Fe(V) was involved. Four different buffer solutions (phosphate (10.0 mM) or bicarbonate (10.0, 100.0, or 250.0 mM)) were used to understand how Fe(V) generated in situ from Fe(VI) oxidation of ABTS might behave differently with different buffer ions. In 10.0 mM phosphate buffer, the stoichiometry between Fe(VI), ABTS, and $ABTS^{\bullet+}$ was 1:1.06:0.99 (Figure S9), which agreed well with the expected 1:1:1.[57,59] Interestingly, the reaction stoichiometry between Fe(VI), ABTS, and $ABTS^{\bullet+}$ was found to be 1:1.25:1.29 (i.e., close to 1:1.3:1.3) in 10.0 mM bicarbonate solution (Figure 4A). This discrepancy with 1:1:1 suggested that bicarbonate-complexed Fe(V) could react with ABTS and generate an equimolar amount of $ABTS^{\bullet+}$ in contrast to the rapid self-decay of phosphate-complexed Fe(V). When the bicarbonate concentration was increased to 100.0 mM (Figure 4B), the stoichiometric ratio between Fe(VI) and ABTS was still larger than 1. However, $ABTS^{\bullet+}$ generation was comparatively lower than ABTS consumption, especially at higher Fe(VI) concentrations, and this phenomenon became even more pronounced when bicarbonate concentration was increased to 250.0 mM (Figure 4C). The above results suggested that bicarbonate-complexed Fe(V) continued to shift its reactivity from H_2O to ABTS or (and) $ABTS^{\bullet+}$, which subsequently generated a transparent ABTS product ($ABTS_{oxidized}$).

Complexation of Fe(VI) and SAs. Fe(VI) complexation with amines and hydroxylamines was investigated by Hornstein,[60] which first identified the intermediary Fe(VI)−imido complex quickly formed during Fe(VI) oxidation of aniline using UV−vis spectrophotometry. Later, Zimmermann[61] examined the efficiency of Fe(VI) oxidation of a range of organic micropollutants and their model compounds. They discovered that SMX and aniline showed a much stronger pH dependence with the oxidation rate constant (k) increasing by more than 4 orders of magnitude when pH was decreased from 11.0 to 5.0, which could not be explained by the speciation variation of SMX and aniline according to their pKa values. Instead, they proposed an Fe(VI)-NH_2-R intermediate complex quickly formed before actual oxidation occurred, and new acid−base equilibria were assigned to these complexes with new pK_a values in order to explain their new speciation behavior. Sharma et al.[62] tried to use Mossbauer spectroscopy to directly detect the intermediate complexation between Fe(VI) and SMX or aniline. However, the Mossbauer spectroscopy of frozen sample in mixed reaction solution in 10 s cannot differentiate the complexed/uncomplexed forms of Fe(VI) if there is no valence-state change. As a result, there was no direct evidence of this complex formation.

In this study, the complexation of Fe(VI) and SAs was observed at 390 nm using UV−vis spectrophotometry. The complexation constants (K) were calculated using the Benesi−Hildebrand equation (eqs 4 and 5) based on the measured

DOI: 10.1021/acs.est.9b00006
Environ. Sci. Technol. 2019, 53, 5272−5281

differences in absorbance (A) and molar absorptivity (ε).[63,64] A detailed complexation titration study is described in Text S4.

$$\frac{1}{\Delta A} = \frac{1}{\Delta\varepsilon[\mathrm{Fe(VI)}]_t K_{1:2}} \frac{1}{[\mathrm{SA}]^2} + \frac{1}{\Delta\varepsilon[\mathrm{Fe(VI)}]_t} \quad (4)$$

$$\frac{1}{\Delta A} = \frac{1}{\Delta\varepsilon[\mathrm{Fe(VI)}]_t K_{1:1}} \frac{1}{[\mathrm{SA}]} + \frac{1}{\Delta\varepsilon[\mathrm{Fe(VI)}]_t} \quad (5)$$

where

$$\Delta\varepsilon = \varepsilon(\mathrm{Fe(VI) + SA}) - \varepsilon(\mathrm{SA}) - \varepsilon(\mathrm{Fe(VI)}) \quad (6)$$

The complexation of Fe(VI) and SAs was observed in Figure S11. In the absence of bicarbonate, the complexation ratio for Fe(VI)/SA was 1:2 for all three SAs, since the linear relationship was only obtained in the form of eq 4. The complexation constants $K_{1:2}$ were determined to be 7.7×10^5 M^{-2} for SMX−Fe(VI)−SMX, 3.1×10^7 M^{-2} for SMZ−Fe(VI)−SMZ, and 1.41×10^6 M^{-2} for SFZ−Fe(VI)−SFZ (Table 1).

Table 1. Complexation Constant K, Molar Absorptivity ε, and Complexation Ratio between Fe(VI) and SAs in the Absence and Presence of Bicarbonate at pH 9.0

	Fe(VI) complexation with SAs		Fe(VI) complexation with SAs in the presence of bicarbonate[a]		
	$K_{1:2}$ (M^{-2})	ε(SA-Fe(VI)-SA) at 390 nm ($M^{-1}\cdot cm^{-1}$)	bicarbonate (M)	$K_{1:1}$ (M^{-1})	ε(Fe(VI)-SA) at 390 nm ($M^{-1}\cdot cm^{-1}$)
SMX	7.70×10^5	977	0.05	166	1722
SMZ	3.10×10^7	387	0.05	275	1257
SFZ	1.41×10^6	528	0.25	26	552

[a]0.05 M total bicarbonate for SMX and SMZ; 0.25 M total bicarbonate for SFZ.

Complexation of Fe(VI) and SAs behaved differently in the presence of bicarbonate (Figure S12). The complexation ratio of Fe(VI)/SA changed from 1:2 to 1:1 when the bicarbonate concentration was increased from 0 to 0.05 M for SMX and SMZ and to 0.25 M for SFZ. The complexation constants $K_{1:1}$ were determined using eq 5. As Table 1 shows, Fe(VI)−SFZ complex displayed the smallest $K_{1:1}$ value (26 M^{-1}), in comparison to the other two complexes (166 M^{-1} for Fe(VI)−SMX and 275 M^{-1} for Fe(VI)−SMZ), indicating the weakest complexation between Fe(VI) and SFZ in the presence of bicarbonate. This result was also consistent with the fact that bicarbonate enhancement effect was shown at a higher bicarbonate concentration for SFZ compared to the other two SAs (Figure 2B).

Proposed Mechanism for the Bicarbonate Enhancement Effect. On the basis of all of the results obtained, it is hypothesized that bicarbonate likely competes with SA for one coordinative site of Fe(VI), thereby reducing the number of SA molecules complexed to Fe(VI) from 2 to 1. Moreover, bicarbonate-complexed Fe(VI) will undergo one-electron transfer to produce bicarbonate-complexed Fe(V) and anilino radical[49] upon oxidation of SAs. A few studies have demonstrated that ligand species will affect high-valent iron species (Fe(V) or Fe(IV)) reactivity to the substrate.[65−68] It is also worthwhile to note that permanganate (Mn(VII)), a similar hypervalent transition-metal oxidant to Fe(VI), showed enhanced reactivity to triclosan[69] and phenolic compounds[70] in the presence of selected ligands (e.g., phosphate, EDTA, and humic acids) because these highly active aqueous manganese intermediates (e.g., Mn(III)) formed in situ upon Mn(VII) reduction) were stabilized by complexation with the ligands via lowered Mn(III)/Mn(II) redox potential. Otherwise, these active manganese intermediates would disproportionate spontaneously in the absence of ligands. Therefore, it is very likely that bicarbonate can also stabilize the intermediate Fe(V) species produced from Fe(VI) via complexation and reducing redox potential and prolonging Fe(V)'s lifetime, thereby preventing rapid spontaneous self-decomposition of Fe(V) and facilitating oxidation rate of SAs. Significantly, experimental studies have shown higher stability of Fe(IV)−carbonate complex than that of Fe(IV)−pyrophosphate complex.[71,72] Furthermore, the hypothesis proposed herein can also be supported by the previous discussion of ABTS oxidation by bicarbonate-complexed Fe(V) and extremely high self-decay rate constant of Fe(V) found in phosphate/borate buffered systems (i.e., 1.5×10^7 M^{-1} s^1).[73]

Additional experiments involving *p*-toluidine and *N,N*-dimethylaniline (DMA) were conducted to investigate the aniline-specific enhancement effect from bicarbonate-complexed Fe(V). As shown by the comparison of empirical rate constants in Figure S13, a similar but even stronger enhancement effect was observed for *p*-toluidine in the presence of bicarbonate while there was no obvious enhancement effect for DMA. This can be explained by the selectivity of bicarbonate-complexed Fe(V) oxidation toward aromatic primary amine. The aromatic primary amine group in *p*-toluidine is activated by the electron-donating methyl group at the *para* position and becomes even more reactive toward bicarbonate-complexed Fe(V). On the other hand, the aromatic primary amine in DMA is substituted with two methyl groups, which obstructs the reaction to bicarbonate-complexed Fe(V) due to the steric hindrance effect. The above statement can also be supported by the fact that the bicarbonate enhancement effect was only observed in SAs (containing aniline) among the few pharmaceuticals chosen in this study. A previous study also reported that Fe(V)'s reactivities with amino acids (e.g., glycine, alaine and aspartic) were 3−5 orders of magnitude higher than those with α-hydroxy acids and organic acids with α-CH_2 groups,[74] which indicates that Fe(V) is a selective oxidant toward amine-specific structures. Considering the bicarbonate stabilizing effect on Fe(V), bicarbonate-complexed Fe(V) is more likely to oxidize more reactive amine species such as aromatic primary amines.

An attempt was made to capture the stabilized Fe(V)'s spectra in the bicarbonate-buffered system using stopped-flow UV−vis spectrophotometry. According to Figure S14, the characteristic peak of Fe(V) at 380 nm[73] was not observed within 0.01−0.1 s. It is likely because bicarbonate ion will not increase the stability of Fe(V) to be longer than the dead time of the stopped-flow instrument (i.e., 0.01 s). Even though there is no direct evidence of bicarbonate stabilization effect on iron/manganese intermediate species owing to their very short lifetime, a few studies found similar phenomenon in bicarbonate−Fe(II)[75−78] and bicarbonate−Mn(II)[78,79] complex systems, where bicarbonate ligand lowered the Fe(III)/Fe(II) redox potential from 0.77 V (vs NHE) to 0.085 V (vs NHE) and the Mn(III)/Mn(II) redox potential from 1.19 V (vs NHE) to 0.63 V (vs NHE). Moreover, similar bicarbonate

DOI: 10.1021/acs.est.9b00006
Environ. Sci. Technol. 2019, 53, 5272−5281

enhancement effect was observed during Mn(VII) oxidation of bisphenol A.[80]

Additionally, potential generation of other iron intermediate species (e.g., Fe(IV)) during the reaction that may also contribute to the degradation of SMX cannot be completely ruled out at this time. Therefore, more research is needed to delineate the role of Fe(IV) in Fe(VI)+bicarbonate system.

Environmental Significance. The extensive occurrence of pharmaceuticals in the aquatic environment and potable water supplies demands more efficient treatment of these micropollutants from the urine source. Unlike the strong scavenging effects of chloride, ammonium and bicarbonate in SHU on $^{\bullet}OH$- and $SO_4^{\bullet-}$-based AOPs (e.g., indirect photolysis of TMP by UV/H_2O_2 and UV/PDS was decreased by ~4 times in SHU without organic metabolites compared to that in PB9)[15,16] and ozonation[14] from previous studies, Fe(VI) application in degrading pharmaceuticals in SHU showed promising results by displaying mild inhibitory effect from chloride and an enhancement effect from ammonium (when the [Fe(VI)]/[ammonium] ratio is ≥0.0012) and bicarbonate. Moreover, this study is among the first to identify and analyze the enhancement effect of bicarbonate on Fe(VI) oxidation of sulfonamides. EPR study excluded the generation of $CO_3^{\bullet-}$ in the Fe(VI) + bicarbonate system. The stoichiometry study between Fe(VI), ABTS, and $ABTS^{\bullet+}$ revealed distinctively different reactivities between bicarbonate-complexed Fe(V) and phosphate-complexed Fe(V). This new finding not only casts doubts on the ABTS spectrophotometric method for Fe(VI) determination in bicarbonate buffer solutions but also sheds light on active iron intermediate species (Fe(V)) using bicarbonate to achieve unexpected enhanced oxidation rate. Overall, the effective destruction of pharmaceuticals in urine at the source using Fe(VI) could be an attractive option to minimize energy-intensive treatment required at centralized wastewater facilities to remove these micropollutants and reduce their potential ecological harm in environmental waters and drinking water. However, to comprehensively understand the performance of Fe(VI) oxidation of pharmaceuticals in hydrolyzed human urine, more research is needed to investigate other urine constituents to fill the gap between synthetic urine and real urine and to validate the removal efficacy of Fe(VI) in real urine samples.

■ ASSOCIATED CONTENT

Supporting Information

The Supporting Information is available free of charge on the ACS Publications website at DOI: 10.1021/acs.est.9b00006.

Text S1−S4, information on chemicals and experimental procedures; Table S1, chemical properties of structures of compounds investigated in this study; Table S2, hydrolyzed urine recipe; Table S3, observed and empirical rate constants with/without chloride ion; Table S4, analysis data of SMX and its OPs; Figure S1−S3, the effects of ammonium and urine matrix on Fe(VI) oxidation; Figure S4, EPR analysis of the carbonate radical; Figure S5, the stoichiometry data and Fe(II) determination; Figure S6−S7, OPs evolution data based peak area; Figure S8, mass spectra of SMX and its OPs; Figure S9, stoichiometries between Fe(VI), ABTS and $ABTS^{\bullet+}$ in 10.0 mM phosphate buffer; Figure S10, SMX and free Fe(VI) loss within 15 s during the complexation; Figures S11 and S12, complexation of SAs and Fe(VI) in the presence/absence of bicarbonate. Figure S13, degradation of *p*-toluidine (A) and DMA (B) by Fe(VI) with and without bicarbonate; Figure S14, stopped-flow UV−vis spectra of Fe(VI) and SMX in the presence of 0.25 M bicarbonate (PDF)

■ AUTHOR INFORMATION

Corresponding Authors

*E-mail: vsharma@sph.tamhsc.edu.
*E-mail: ching-hua.huang@ce.gatech.edu.

ORCID

Virender K. Sharma: 0000-0002-5980-8675
Ching-Hua Huang: 0000-0002-3786-094X

Notes

The authors declare no competing financial interest.

■ ACKNOWLEDGMENTS

This work was supported by the projects from the National Science Foundation (CBET 1802944 and CBET 1802800).

■ REFERENCES

(1) CDC (Centers for Disease Control and Prevention). *National Ambulatory Medical Care Survey: 2014 State and National Summary Tables*; 2017. Available from: http://www.cdc.gov/nchs/ahcd/ahcd_products.htm.

(2) Calero-Cáceres, W.; Melgarejo, A.; Colomer-Lluch, M.; Stoll, C.; Lucena, F.; Jofre, J.; Muniesa, M. Sludge as a potential important source of antibiotic resistance genes in both the bacterial and bacteriophage fractions. *Environ. Sci. Technol.* **2014**, *48* (13), 7602−7611.

(3) Lienert, J.; Bürki, T.; Escher, B. I. Reducing micropollutants with source control: substance flow analysis of 212 pharmaceuticals in faeces and urine. *Water Sci. Technol.* **2007**, *56* (5), 87−96.

(4) Meinzinger, F.; Oldenburg, M. Characteristics of source-separated household wastewater flows: a statistical assessment. *Water Sci. Technol.* **2009**, *59* (9), 1785−1791.

(5) Larsen, T. A.; Gujer, W. Separate management of anthropogenic nutrient solutions (human urine). *Water Sci. Technol.* **1996**, *34* (3−4), 87−94.

(6) Jönsson, H.; Vinnerås, B. Experiences and suggestions for collection systems for source-separated urine and faeces. *Water Sci. Technol.* **2007**, *56* (5), 71−76.

(7) Rossi, L.; Lienert, J.; Larsen, T. Real-life efficiency of urine source separation. *J. Environ. Manage.* **2009**, *90* (5), 1909−1917.

(8) Mobley, H.; Hausinger, R. Microbial ureases: significance, regulation, and molecular characterization. *Microbiol. Rev.* **1989**, *53* (1), 85−108.

(9) Pronk, W.; Palmquist, H.; Biebow, M.; Boller, M. Nanofiltration for the separation of pharmaceuticals from nutrients in source-separated urine. *Water Res.* **2006**, *40* (7), 1405−1412.

(10) Landry, K. A.; Boyer, T. H. Diclofenac removal in urine using strong-base anion exchange polymer resins. *Water Res.* **2013**, *47* (17), 6432−6444.

(11) Landry, K. A.; Sun, P.; Huang, C.-H.; Boyer, T. H. Ion-exchange selectivity of diclofenac, ibuprofen, ketoprofen, and naproxen in ureolyzed human urine. *Water Res.* **2015**, *68*, 510−521.

(12) Escher, B. I.; Pronk, W.; Suter, M. J. F.; Maurer, M. Monitoring the removal efficiency of pharmaceuticals and hormones in different treatment processes of source-separated urine with bioassays. *Environ. Sci. Technol.* **2006**, *40* (16), 5095−5101.

(13) Solanki, A.; Boyer, T. H. Pharmaceutical removal in synthetic human urine using biochar. *Environmental Science: Water Sci. Technol.* **2017**, *3* (3), 553−565.

(14) Dodd, M. C.; Zuleeg, S.; Von Gunten, U.; Pronk, W. Ozonation of source-separated urine for resource recovery and waste

DOI: 10.1021/acs.est.9b00006
Environ. Sci. Technol. 2019, 53, 5272−5281

minimization: Process modeling, reaction chemistry, and operational considerations. *Environ. Sci. Technol.* **2008**, *42* (24), 9329−9337.
(15) Zhang, R.; Sun, P.; Boyer, T. H.; Zhao, L.; Huang, C. H. Degradation of pharmaceuticals and metabolite in synthetic human urine by UV, UV/H_2O_2, and UV/PDS. *Environ. Sci. Technol.* **2015**, *49* (5), 3056−3066.
(16) Zhang, R.; Yang, Y.; Huang, C.-H.; Li, N.; Liu, H.; Zhao, L.; Sun, P. UV/H_2O_2 and UV/PDS treatment of trimethoprim and sulfamethoxazole in synthetic human urine: Transformation products and toxicity. *Environ. Sci. Technol.* **2016**, *50* (5), 2573−2583.
(17) Goodwill, J. E.; Jiang, Y.; Reckhow, D. A.; Gikonyo, J.; Tobiason, J. E. Characterization of particles from ferrate preoxidation. *Environ. Sci. Technol.* **2015**, *49* (8), 4955−4962.
(18) Goodwill, J. E.; Jiang, Y.; Reckhow, D. A.; Tobiason, J. E. Laboratory Assessment of Ferrate for Drinking Water Treatment. *J. Am. Water Works Assoc.* **2016**, *108* (3), E164−E174.
(19) Karlesa, A.; De Vera, G. A. D.; Dodd, M. C.; Park, J.; Espino, M. P. B.; Lee, Y. Ferrate (VI) oxidation of β-lactam antibiotics: Reaction kinetics, antibacterial activity changes, and transformation products. *Environ. Sci. Technol.* **2014**, *48* (17), 10380−10389.
(20) Sharma, V. K.; Anquandah, G. A.; Nesnas, N. Kinetics of the oxidation of endocrine disruptor nonylphenol by ferrate(VI). *Environ. Chem. Lett.* **2009**, *7* (2), 115−119.
(21) Anquandah, G. A.; Sharma, V. K.; Knight, D. A.; Batchu, S. R.; Gardinali, P. R. Oxidation of trimethoprim by ferrate(VI): kinetics, products, and antibacterial activity. *Environ. Sci. Technol.* **2011**, *45* (24), 10575−10581.
(22) Anquandah, G. A.; Sharma, V. K.; Panditi, V. R.; Gardinali, P. R.; Kim, H.; Oturan, M. A. Ferrate (VI) oxidation of propranolol: kinetics and products. *Chemosphere* **2013**, *91* (1), 105−109.
(23) Yang, B.; Ying, G.-G.; Zhao, J.-L.; Liu, S.; Zhou, L.-J.; Chen, F. Removal of selected endocrine disrupting chemicals (EDCs) and pharmaceuticals and personal care products (PPCPs) during ferrate(VI) treatment of secondary wastewater effluents. *Water Res.* **2012**, *46* (7), 2194−2204.
(24) Hu, L.; Martin, H. M.; Arce-Bulted, O.; Sugihara, M. N.; Keating, K. A.; Strathmann, T. J. Oxidation of carbamazepine by Mn(VII) and Fe(VI): Reaction kinetics and mechanism. *Environ. Sci. Technol.* **2009**, *43* (2), 509−515.
(25) Zimmermann, S. G.; Schmukat, A.; Schulz, M.; Benner, J.; von Gunten, U.; Ternes, T. A. Kinetic and mechanistic investigations of the oxidation of tramadol by ferrate and ozone. *Environ. Sci. Technol.* **2012**, *46*, 876−884.
(26) Lee, Y.; Zimmermann, S. G.; Kieu, A. T.; von Gunten, U. Ferrate (Fe(VI)) application for municipal wastewater treatment: A novel process for simultaneous micropollutant oxidation and phosphate removal. *Environ. Sci. Technol.* **2009**, *43*, 3831−3838.
(27) Neta, P.; Huie, R. E.; Ross, A. B. *Rate Constants for Reactions of Inorganic Radicals in Aqueous Solution*; American Chemical Society and the American Institute of Physics for the National Bureau of Standards, 1988.
(28) Sharma, V. K.; Bloom, J. T.; Joshi, V. N. Oxidation of ammonia by ferrate (VI). *J. Environ. Sci. Health, Part A: Toxic/Hazard. Subst. Environ. Eng.* **1998**, *33* (4), 635−650.
(29) Huang, L.; Li, L.; Dong, W.; Liu, Y.; Hou, H. Removal of Ammonia by OH Radical in Aqueous Phase. *Environ. Sci. Technol.* **2008**, *42* (21), 8070−8075.
(30) Jiang, Y.; Goodwill, J. E.; Tobiason, J. E.; Reckhow, D. A. Effect of different solutes, natural organic matter, and particulate Fe(III) on ferrate(VI) decomposition in aqueous solutions. *Environ. Sci. Technol.* **2015**, *49* (5), 2841−2848.
(31) Norcross, B. E.; Lewis, W. C.; Gai, H.; Noureldin, N. A.; Lee, D. G. The oxidation of secondary alcohols by potassium tetraoxoferrate(VI). *Can. J. Chem.* **1997**, *75* (2), 129−139.
(32) Sharma, V. K. Potassium ferrate(VI): an environmentally friendly oxidant. *Adv. Environ. Res.* **2002**, *6* (2), 143−156.
(33) Hughes, S. R.; Kay, P.; Brown, L. E. Global synthesis and critical evaluation of pharmaceutical data sets collected from river systems. *Environ. Sci. Technol.* **2013**, *47* (2), 661−677.
(34) Benotti, M. J.; Trenholm, R. A.; Vanderford, B. J.; Holady, J. C.; Stanford, B. D.; Snyder, S. A. Pharmaceuticals and endocrine disrupting compounds in US drinking water. *Environ. Sci. Technol.* **2009**, *43* (3), 597−603.
(35) Zhang, T.; Li, B. Occurrence, transformation, and fate of antibiotics in municipal wastewater treatment plants. *Crit. Rev. Environ. Sci. Technol.* **2011**, *41* (11), 951−998.
(36) Saude, E. J.; Sykes, B. D. Urine stability for metabolomic studies: Effects of preparation and storage. *Metabolomics* **2007**, *3* (1), 19−27.
(37) Yang, C.; Liu, H.; Li, M.; Yu, C. Treating urine by *Spirulina platensis*. *Acta Astronaut.* **2008**, *63* (7), 1049−1054.
(38) Feng, M.; Jinadatha, C.; McDonald, T. J.; Sharma, V. K. Accelerated Oxidation of Organic Contaminants by Ferrate(VI): The Overlooked Role of Reducing Additives. *Environ. Sci. Technol.* **2018**, *52* (19), 11319−11327.
(39) Carr, J. D.; Kelter, P. B.; Tabatabai, A.; Splichal, D.; Erickson, J.; McLaughlin, C. Properties of ferrate(VI) in aqueous solution: an alternate oxidant in wastewater treatment. In *Proceedings of Conference on Water Chlorination: Environmental Impact and Health Effects*; Jolley, R. L., Eds.; Lewis: Chelsea, MI, 1985; pp 1285−1298.
(40) Sharma, V. K.; Burnett, C. R.; Millero, F. J. Dissociation constants of the monoprotic ferrate (VI) ion in NaCl media. *Phys. Chem. Chem. Phys.* **2001**, *3* (11), 2059−2062.
(41) Sharma, V. K.; Mishra, S. K.; Ray, A. K. Kinetic assessment of the potassium ferrate(VI) oxidation of antibacterial drug sulfamethoxazole. *Chemosphere* **2006**, *62* (1), 128−134.
(42) Feng, M.; Cizmas, L.; Wang, Z.; Sharma, V. K. Activation of ferrate(VI) by ammonia in oxidation of flumequine: Kinetics, transformation products, and antibacterial activity assessment. *Chem. Eng. J.* **2017**, *323*, 584−591.
(43) Collins, T. J.; Ryabov, A. D. Targeting of high-valent iron-TAML activators at hydrocarbons and beyond. *Chem. Rev.* **2017**, *117* (13), 9140−9162.
(44) Nam, W.; Lee, Y.-M.; Fukuzumi, S. Hydrogen atom transfer reactions of mononuclear nonheme metal−oxygen intermediates. *Acc. Chem. Res.* **2018**, *51* (9), 2014−2022.
(45) Chen, S.-N.; Hoffman, M. Z. Rate constants for the reaction of the carbonate radical with compounds of biochemical interest in neutral aqueous solution. *Radiat. Res.* **1973**, *56* (1), 40−47.
(46) Sharma, V. K.; Mishra, S. K.; Nesnas, N. Oxidation of sulfonamide antimicrobials by ferrate (VI)[$Fe^{VI}O_4^{2-}$]. *Environ. Sci. Technol.* **2006**, *40* (23), 7222−7227.
(47) Dodd, M. C.; Huang, C.-H. Transformation of the antibacterial agent sulfamethoxazole in reactions with chlorine: kinetics, mechanisms, and pathways. *Environ. Sci. Technol.* **2004**, *38* (21), 5607−5615.
(48) Gao, S.; Zhao, Z.; Xu, Y.; Tian, J.; Qi, H.; Lin, W.; Cui, F. Oxidation of sulfamethoxazole (SMX) by chlorine, ozone and permanganate—a comparative study. *J. Hazard. Mater.* **2014**, *274*, 258−269.
(49) Huang, H.; Sommerfeld, D.; Dunn, B. C.; Lloyd, C. R.; Eyring, E. M. Ferrate(VI) oxidation of aniline. *Dalton Trans* **2001**, No. 8, 1301−1305.
(50) Manoli, K.; Nakhla, G.; Ray, A. K.; Sharma, V. K. Oxidation of caffeine by acid-activated ferrate(VI): Effect of ions and natural organic matter. *AIChE J.* **2017**, *63* (11), 4998−5006.
(51) Feng, M.; Sharma, V. K. Enhanced oxidation of antibiotics by ferrate(VI)-sulfur(IV) system: Elucidating multi-oxidant mechanism. *Chem. Eng. J.* **2018**, *341*, 137−145.
(52) Sharma, V. K. Ferrate(VI) and ferrate(V) oxidation of organic compounds: Kinetics and mechanism. *Coord. Chem. Rev.* **2013**, *257* (2), 495−510.
(53) Bielski, B. H. J.; Sharma, V. K.; Czapski, G. Reactivity of ferrate(V) with carboxylic acids: A pre-mix pulse radiolysis study. *Radiat. Phys. Chem.* **1994**, *44* (5), 479−484.
(54) Loegager, T.; Holcman, J.; Sehested, K.; Pedersen, T. Oxidation of ferrous ions by ozone in acidic solutions. *Inorg. Chem.* **1992**, *31* (17), 3523−3529.

DOI: 10.1021/acs.est.9b00006
Environ. Sci. Technol. 2019, 53, 5272−5281

(55) Pinkernell, U.; Lüke, H. J.; Karst, U. Selective photometric determination of peroxycarboxylic acids in the presence of hydrogen peroxide. *Analyst* **1997**, *122* (6), 567−571.
(56) Pinkernell, U.; Nowack, B.; Gallard, H.; Von Gunten, U. Methods for the photometric determination of reactive bromine and chlorine species with ABTS. *Water Res.* **2000**, *34* (18), 4343−4350.
(57) Lee, Y.; Yoon, J.; von Gunten, U. Spectrophotometric determination of ferrate (Fe(VI)) in water by ABTS. *Water Res.* **2005**, *39* (10), 1946−1953.
(58) Lee, Y.; Kissner, R.; von Gunten, U. Reaction of ferrate (VI) with ABTS and self-decay of ferrate (VI): Kinetics and mechanisms. *Environ. Sci. Technol.* **2014**, *48* (9), 5154−5162.
(59) Huang, Z. S.; Wang, L.; Liu, Y. L.; Jiang, J.; Xue, M.; Xu, C. B.; Zhen, Y. F.; Wang, Y. C.; Ma, J. Impact of phosphate on ferrate oxidation of organic compounds: An underestimated oxidant. *Environ. Sci. Technol.* **2018**, *52* (23), 13897−13907.
(60) Hornstein, B. J. *Reaction mechanisms of hypervalent iron: The oxidation of amines and hydroxylamines by potassium ferrate, K2FeO4*; New Mexico State University, 1999.
(61) Zimmermann, S. G. Enhanced wastewater treatment by ozone and ferrate. *Diss., Eidgenössische Technische Hochschule ETH Zürich, Nr.* **19615**, 2011.
(62) Sharma, V. K.; Homonnay, Z.; Siskova, K.; Machala, L.; Zboril, R. Mössbauer investigation of the reaction of ferrate(VI) with sulfamethoxazole and aniline in alkaline medium. *LACAME 2012*; Springer, 2013; 1−7.
(63) Wen, X.; Tan, F.; Jing, Z.; Liu, Z. Preparation and study the 1:2 inclusion complex of carvedilol with β-cyclodextrin. *J. Pharm. Biomed. Anal.* **2004**, *34* (3), 517−523.
(64) Wang, H.; Yao, H.; Sun, P.; Li, D.; Huang, C.-H. Transformation of tetracycline antibiotics and Fe(II) and Fe(III) species induced by their complexation. *Environ. Sci. Technol.* **2016**, *50* (1), 145−153.
(65) Sastri, C. V.; Lee, J.; Oh, K.; Lee, Y. J.; Lee, J.; Jackson, T. A.; Ray, K.; Hirao, H.; Shin, W.; Halfen, J. A.; Kim, J.; Que, L.; Shaik, S.; Nam, W. Axial ligand tuning of a nonheme iron(IV)−oxo unit for hydrogen atom abstraction. *Proc. Natl. Acad. Sci. U. S. A.* **2007**, *104* (49), 19181−19186.
(66) Song, W. J.; Ryu, Y. O.; Song, R.; Nam, W. Oxoiron(IV) porphyrin π-cation radical complexes with a chameleon behavior in cytochrome P450 model reactions. *JBIC, J. Biol. Inorg. Chem.* **2005**, *10* (3), 294−304.
(67) McDonald, A. R.; Que, L., Jr High-valent nonheme iron-oxo complexes: Synthesis, structure, and spectroscopy. *Coord. Chem. Rev.* **2013**, *257* (2), 414−428.
(68) Mills, M. R.; Weitz, A. C.; Hendrich, M. P.; Ryabov, A. D.; Collins, T. J. NaClO-generated iron(IV)oxo and iron(V)oxo TAMLs in pure water. *J. Am. Chem. Soc.* **2016**, *138* (42), 13866−13869.
(69) Jiang, J.; Pang, S.-Y.; Ma, J. Oxidation of triclosan by permanganate (Mn(VII)): Importance of ligands and *in situ* formed manganese oxides. *Environ. Sci. Technol.* **2009**, *43* (21), 8326−8331.
(70) Jiang, J.; Pang, S. Y.; Ma, J. Role of ligands in permanganate oxidation of organics. *Environ. Sci. Technol.* **2010**, *44* (11), 4270−4275.
(71) Melton, J. D.; Bielski, B. H. Studies of the kinetic, spectral and chemical properties of Fe(IV) pyrophosphate by pulse radiolysis. *Radiot. Phys. Chem.* **1990**, *36* (6), 725−733.
(72) Bielski, B. H. [4] Generation of iron(IV) and iron(V) complexes in aqueous solutions. In *Methods in Enzymology*; Elsevier, 1990; Vol. *186*, p 108−113.
(73) Rush, J.; Bielski, B. H. Kinetics of ferrate(V) decay in aqueous solution. A pulse-radiolysis study. *Inorg. Chem.* **1989**, *28* (21), 3947−3951.
(74) Bielski, B. H. J.; Sharma, V. K.; Czapski, G. Reactivity of ferrate(V) with carboxylic acids: A pre-mix pulse radiolysis study. *Radiat. Phys. Chem.* **1994**, *44* (5), 479−484.
(75) Strathmann, T. J.; Stone, A. T. Reduction of oxamyl and related pesticides by Fe^{II}: Influence of organic ligands and natural organic matter. *Environ. Sci. Technol.* **2002**, *36* (23), 5172−5183.
(76) King, D. W.; Farlow, R. Role of carbonate speciation on the oxidation of Fe(II) by H_2O_2. *Mar. Chem.* **2000**, *70* (1), 201−209.
(77) King, D. W. Role of Carbonate speciation on the oxidation rate of Fe(II) in aquatic systems. *Environ. Sci. Technol.* **1998**, *32* (19), 2997−3003.
(78) Kozlov, Y. N.; Zharmukhamedov, S. K.; Tikhonov, K. G.; Dasgupta, J.; Kazakova, A. A.; Dismukes, G. C.; Klimov, V. V. Oxidation potentials and electron donation to photosystem II of manganese complexes containing bicarbonate and carboxylate ligands. *Phys. Chem. Chem. Phys.* **2004**, *6* (20), 4905−4911.
(79) Kozlov, Y.; Kazakova, A.; Klimov, V. Changes in the redox potential and catalase activity of Mn^{2+} ions during formation of Mn-bicarbonate complexes. *Membr. Cell Biol.* **1997**, *11* (1), 115−120.
(80) Zhang, J.; Sun, B.; Guan, X. Oxidative removal of bisphenol A by permanganate: Kinetics, pathways and influences of co-existing chemicals. *Sep. Purif. Technol.* **2013**, *107*, 48−53.

DOI: 10.1021/acs.est.9b00006
Environ. Sci. Technol. 2019, 53, 5272−5281

Supporting Information

Oxidation of Pharmaceuticals by Ferrate(VI) in Hydrolyzed Urine: Effects of Major Inorganic Constituents

Cong Luo,[1] Mingbao Feng,[2] Virender K. Sharma,[2,*] and Ching-Hua Huang[1,*]

[1] School of Civil and Environmental Engineering, Georgia Institute of Technology, Atlanta, Georgia 30332, United States

[2] Department of Environment and Occupational Health, School of Public Health, Texas A&M University, College Station, Texas 77843, United States

*Corresponding Authors.

E-mail: ching-hua.huang@ce.gatech.edu (Ching-Hua Huang)

Email: vsharma@sph.tamhsc.edu (Virender K. Sharma)

Content:

Text S1. Chemicals and Reagents

Carbamazepine (CBZ), naproxen (NAP), sulfamethoxazole (SMX), sulfamethizole (SFZ), sulfamethazine(SMZ), 3,5-dimethylisoxazole (DMI), 3-amino-5-methylisoxazole (AMI), 4-aminophenyl methyl sulfone (APMS), 2,2'-azino-bis(3-ethylbenzothiazoline-6-sulfonate) (ABTS), 1,10-phenanthroline, aniline, and trimethoprim (TMP) were purchased from Sigma-Aldrich. Potassium ferrate(VI) (K_2FeO_4) was synthesized in Dr. Sharma's lab at Texas A&M University (TAMU) and shipped to Georgia Tech (GT). All the chemical standards were of 97% or greater in purity and used directly without further purification. Reagent-grade deionized (DI) water (resistivity > 18 mΩ·cm) was prepared from a Nanopure Millipore (Billerica, MA) water purification system. The stock solutions of individual pharmaceuticals were prepared in phosphate buffer (10.0 mM) at pH 9.0 at concentrations of 50.0 μM (CBZ, NAP), 200.0 μM (TMP), 250.0 μM (DMI, AMI, APMS, aniline), or 800.0 μM (SMX, SMZ, SFZ). The stock solutions were freshly prepared prior to the experiments, stored at 5 °C and used within one week.

Text S2. Analytical Methods

An Agilent 1100 series HPLC system equipped with a UV diode-array detector (DAD) and a Zorbax SB-C18 column (2.1 mm × 150 mm, 5 μm) was used to monitor the loss of parent compounds of pharmaceuticals. Detection wavelengths for SMX, SMZ, SFZ, DMI, AMI, aniline, TMP, CBZ, NAP, and APMS were set at 275, 285, 260, 210, 230, 236, 254, 285, 231 and 205 nm, respectively. Gradient elution was used with (i) 0.1% (v/v) formic acid and methanol for SMX, AMI, CBZ and NAP; and (ii) 0.1% (v/v) formic acid and acetonitrile for TMP, DMI, aniline, SFZ, SMZ, and APMS.

The oxidized products (OPs) of SMX by Fe(VI) in the presence or absence of bicarbonate were identified using solid phase extraction, followed by liquid chromatography-high-resolution/accurate mass (HR/AM) spectrometry (SPE-LC-HRMS) analysis. The reaction solutions withdrawn at certain degradation times were filtered by 0.45 μm glass-fiber filters and then concentrated by a Visiprep SPE apparatus (Supleco, USA) with Waters Oasis HLB cartridges (WAT106202, 6 cc/200 mg). Before extraction, each HLB cartridge was sequentially conditioned with 5 mL methanol and 5 mL water. Then, the cartridge was loaded with 100 mL sample, washed with 5 mL water, and vacuum dried for 5 min. Finally, the extracted degradation products were obtained by eluting the cartridge with 2 × 2 mL methanol. The degradation products were kept in sealed vials and shipped with ice overnight to TAMU, where the samples were analyzed by LC-HRMS. The full-scan analysis of untargeted products was performed on a Q Exactive Plus OrbiTrap mass detector (Thermo Scientific, Waltham, MA) coupled to a binary pump HPLC (Ultimate 3000, Thermo Scientific) in a positive ion mode using an electrospray ion (ESI) source. For data acquisition, the sheath, aux and sweep gasses were set at 50, 10 and 1, respectively. The spray voltage was set to 4 kV, and the S-lens RF was set to 50. The aux gas heater and capillary temperatures were maintained at 375 and 350 °C, respectively. Full MS spectra were obtained at 70,000 resolution (*m/z* 200) with a scan range of *m/z* 50-750. Full MS → ddMS2 scans were obtained at 35,000 resolution (MS1) and 17,500 resolution (MS2) with a 1.5 *m/z* isolation window and a stepped NCE (20, 40, and 60). Samples were maintained at 4 °C before injection. The injection volume was 10 μL. Chromatographic separation was achieved on a Hypersil GOLD^{TM} C_{18} selectivity LC column (50 mm × 2.1 mm, particle size 3 μm) at 25 °C using a solvent gradient method. The mobile phase was water (0.3% formic acid) (A) and methanol (B). The gradient method used was 0-2 min (10% B to 80% B), 2-3 min (90% B to 20% B), 3-26 min (90% B), 26-

27 min (10% B), and 27-35 min (10% B). The flow rate was 0.2 mL/min. Sample acquisition was performed by Xcalibur (Thermo Scientific). The high-resolution MS data were processed using Compound Discoverer 2.1 software (Thermo Scientific) and online molecular structure libraries (i.e., *m/z* cloud and ChemSpider).

The room-temperature electron paramagnetic resonance (EPR) experiments were performed at room temperature using a Bruker ELEXSYS-II E500 spectrometer (Rheinstetten, Germany) at the X-band frequency of 9.4 GHz. The reaction solutions were pre-added with DMPO (100.0 mM), and then transferred to 2 mm EPR tube for the carbonate radical measurements.[1] The related operating parameters were selected: center field, 3340.0 G; sweep width, 160.0 G; sweep time, 30 s; attenuation, 25.0 dB; scan times, 10.

The stopped-flow spectrophotometer (Applied Photophysics SX-20 MV, Surrey, UK) coupled with photodiode array (PDA) detector was used to try to capture the Fe(V) spectra and the total reaction time was selected in the range of 0.1 s to 1000 s. The UV-vis spectral measurements were performed on the reaction solutions containing 300.0 μM Fe(VI) and 10.0 μM SMX at pH 9.0 (10.0 mM phosphate buffer) with or without 0.25 M bicarbonate.

Text S3. Reaction Stoichiometry Study

Reaction between Fe(VI) and SMX. The reaction stoichiometric molar ratio of SMX and Fe(VI) in the presence of 0.25 M bicarbonate was determined by mixing different amounts of stock solutions of SMX and Fe(VI) into the 0.25 M bicarbonate solution that was maintained at pH 9.0 using phosphate buffer (PB). The stock solutions of SMX and Fe(VI) were both prepared in 10.0 mM PB at pH 9.0 in the presence of 0.25 M bicarbonate. The concentration of SMX was fixed at 100.0 μM, while Fe(VI) concentration varied from 100.0 to 600.0 μM. It is important to point out

that Fe(VI) could also react with bicarbonate and phosphate buffer in water; thus, Fe(VI) and buffered solution with 0.25 M bicarbonate were also mixed together to monitor the self-decay of Fe(VI). The amount of Fe(VI) reacted with SMX only can be obtained accordingly by subtracting the self-decay of Fe(VI). Fe(VI) concentration was determined at 508 nm ($\varepsilon(FeO_4^{2-}$, 510 nm) = 1.03×10^3 cm^{-1} M^{-1}) with UV-visible spectrophotometry.

Reaction between Fe(VI) and ABTS. The reaction stoichiometric molar ratio of ABTS and Fe(VI) was studied in 10.0 mM phosphate buffer, or in 10.0 mM, 100.0 mM and 250.0 mM bicarbonate solution, respectively. All solutions were at pH 9.0. Experiments were conducted by adding a constant amount (1.0 mL) of ABTS stock solution into varied concentrations of Fe(VI) solutions (25.0 mL). The Fe(VI) solutions were prepared in the above different types of buffer solutions (with phosphate or bicarbonate) at 5.0-25.0 μM of Fe(VI). The ABTS stock solution was at an excess concentration of 2.5 mM prepared in DI water with NaOH to make sure the initial pH maintained at 9.0. Formation of $ABTS^{\bullet+}$ was monitored at 415 nm ($\varepsilon(ABTS^{\bullet+}$, 415nm) = 3.4×10^4 cm^{-1} M^{-1}) with UV-visible spectrophotometry. The consumption of ABTS was determined at 340 nm (ε(ABTS, 340 nm) = 3.66×10^4 cm^{-1} M^{-1}, $\varepsilon(ABTS^{\bullet+}$, 340 nm) = 5.4×10^3 cm^{-1} M^{-1}) after the reaction, and then the concentrations were calculated according to the methods proposed in a previous study.[2]

Text S4. Determination of Complexation Ratio and Constants for Fe(VI)+SA complexes

The Fe(VI) and SA complexation was detected by the difference in the UV absorbance of the Fe(VI)+SA complex in comparison to the UV absorbance of the free Fe(VI) plus that of free SA at 390 nm, as shown by the equation (1) below:

$$\Delta(\text{absorbance}) = Abs^{(Fe(VI)+SA)} - Abs^{(Fe(VI)\ only)} - Abs^{(SA\ only)} \quad (1)$$

The complexation reaction may be expressed in two ways as below:

$$\text{Fe(VI)} + \text{SA} = \text{Fe(VI)-SA} \qquad K_{1:1} = [\text{Fe(VI)-SA}]/([\text{Fe(VI)}][\text{SA}]) \qquad (2)$$

$$\text{Fe(VI)} + 2\ \text{SA} = \text{SA-Fe(VI)-SA} \qquad K_{1:2} = [\text{SA-Fe(VI)-SA}]/([\text{Fe(VI)}][\text{SA}]^2) \qquad (3)$$

where Fe(VI) and SA are individually the concentrations of uncomplexed Fe(VI) and SA, and $K_{1:1}$ and $K_{1:2}$ are the 1:1 and 1:2 complexation constants, respectively.

To determine the complexation constant K, the Δ(absorbance) was measured in a complexometric titration with affixed total Fe(VI) concentration but varying SA concentrations. The results were applied to the Benesi-Hildebrand equation to obtain the value $K_{1:1}$[3] by plotting 1/[SA] versus 1/Δ(absorbance) and the value of $K_{1:2}$[4] by plotting $1/[\text{SA}]^2$ versus 1/Δ (absorbance) according to the following equations:

$$\frac{1}{\Delta A} = \frac{1}{\Delta\varepsilon\,[\text{Fe(VI)}]_t\, K_{1:2}}\frac{1}{[\text{SA}]^2} + \frac{1}{\Delta\varepsilon\,[\text{Fe(VI)}]_t} \qquad (4)$$

$$\frac{1}{\Delta A} = \frac{1}{\Delta\varepsilon\,[\text{Fe(VI)}]_t\, K_{1:1}}\frac{1}{[\text{SA}]} + \frac{1}{\Delta\varepsilon\,[\text{Fe(VI)}]_t} \qquad (5)$$

$$\text{where} \quad \Delta\varepsilon = \varepsilon(\text{Fe(VI)+SA}) - \varepsilon(\text{SA}) - \varepsilon(\text{Fe(VI)}) \qquad (6)$$

Δ(Absorbance) was the difference in the UV absorbance of the Fe(VI)+SA complex in comparison to the UV absorbance of the uncomplexed Fe(VI) plus that of uncomplexed SA; Fe(VI)_t was the total Fe(VI) concentration; and $\Delta\varepsilon = \varepsilon(\text{Fe(VI)+SA}) - \varepsilon(\text{Fe(VI)}) - \varepsilon(\text{SA})$ (the molar absorptivity of Fe(VI)+SA complex minus the absorptivities of uncomplexed Fe(VI) and uncomplexed SA). By plotting 1/[SA] versus 1/Δ(Absorbance), the complexation constant $K_{1:1}$ could be calculated from dividing the intercept by the slope. By plotting $1/[\text{SA}]^2$ versus 1/Δ(Absorbance), the complexation constant $K_{1:2}$ could be calculated from dividing the intercept by the slope. Complexometric titration experiments were conducted at a fixed Fe(VI)_t (100.0 μM) with varying [SA] (0 – 600.0 μM) (assuming $[\text{SA}] \approx [\text{SA}]_0$, because $[\text{Fe(VI)+SA}] \ll [\text{SA}]$).

The absorbance was measured within 15 s immediately after Fe(VI) and SA was mixed together for complexation. Preliminary study of SMX loss within 15 s was conducted to exclude the possible interference of SA degradation products by monitoring the absorbance increase at 390 nm. From Figure S10, less than 2% SMX loss was observed under varying [SMX]:[Fe(VI)] ratios within 15 s. This suggested that the degradation of SA with 15 s was negligible. In contrast, free Fe(VI) concentration, detected at 508 nm, decreased significantly as the initial SMX concentration was increased, indicating that Fe(VI)-SMX complex started to accumulate to some degree since the self-decay of Fe(VI) is very minimum at pH 9.0 within 15 s ($t_{1/2}$ = 4.83 hr).[5]

Table S1. Chemical properties and structures of compounds investigated in this study.

	Formula	Mol. Weight	p*K*a	Structure
Sulfamethoxazole (SMX)	$C_{10}H_{11}N_3O_3S$	253.3	pK_{a1} = 1.7 pKa$_2$ = 5.89	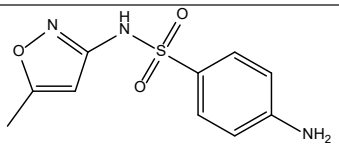
Trimethoprim (TMP)	$C_{14}H_{18}N_4O_3$	290.3	pKa$_1$ = 3.2 pKa$_2$ = 7.1	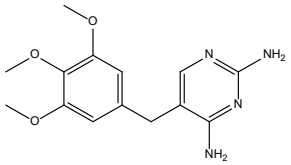
Carbamazepine (CBZ)	$C_{14}H_{12}N_2O$	236.3	pKa$_1$ = 7 pKa$_2$ = 13.9	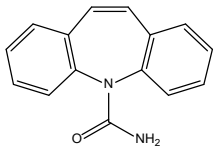
Naproxen (NAP)	$C_{14}H_{14}O_3$	230.3	pKa = 4.2	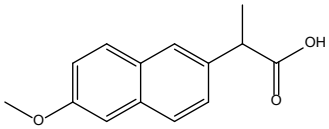
Sulfamethazine (SMZ)	$C_{12}H_{14}N_4O_2S$	278.3	pK_{a1} = 2.3 pKa$_2$ = 7.4	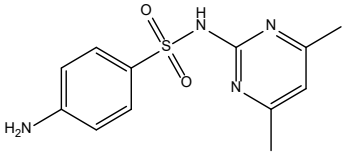
Sulfamethizole (SFZ)	$C_9H_{10}N_4O_2S_2$	270.3	pK_{a1} = 2.1 pKa$_2$ = 5.3	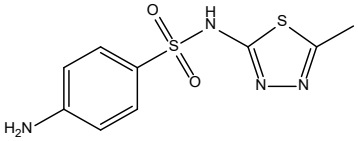
3,5-dimethylisoazole (DMI)	C_5H_7NO	97.1	Not Available	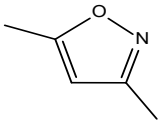
3-amino-5-methylisoxazole (AMI)	$C_4H_6N_2O$	98.1	Not Available	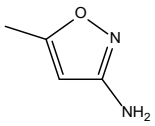
4-aminophenyl methyl sulfone (APMS)	$C_7H_9NO_2S$	171.2	Not Available	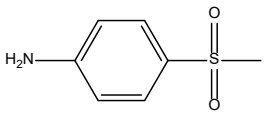
Aniline	C_6H_7N	93.1	pKa = 4.63	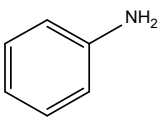

2,2'-azino-bis(3-ethylbenzothiazoline-6-sulphonic acid) (ABTS)	$C_{18}H_{18}N_4O_6S_4$	514.7	p*K*a = 2.08	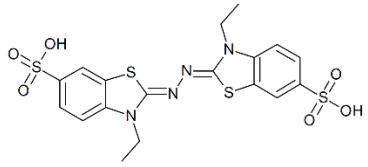
***p*-toluidine**	C_7H_9N	107.1	p*K*a = 5.10	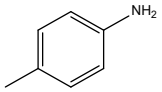
***N,N*-dimethylaniline (DMA)**	C_8HN	121.1	p*K*a = 5.15	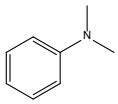

Table S2. The composition of synthetic hydrolyzed urine (SHU) (pH 9.0).

	M.W. (g/mol)	Concentration (mM)
Creatinine	113.12	7.40
Creatine	131.13	1.38
Hippuric acid (HA)	179.17	0.17
NaCl	58.44	60.00
Na_2SO_4	142.04	15.00
KCl	74.55	40.00
NH_4OH	35.04	250.00
NaH_2PO_4	119.98	13.60
NH_4HCO_3	79.06	250.00
$NaHCO_3$	84.01	250.00

Note: To prepare NH_3-Free SHU, $NaHCO_3$ was used to substitute NH_4HCO_3 and NH_4OH was not added.

Table S3. Comparison of the observed (R^2 = 0.987 – 0.996) and empirical rate constants with/without chloride ion.

	[Cl^-] = 0.0 M		**[Cl^-] = 0.1 M**		**Difference (%) in empirical rate constants with/without Cl^-**
	Observed Rate Constant k_{obs}, (min^{-1})	**Empirical Rate Constant $k_{obs}/\alpha(HFeO_4^-)$, (min^{-1})**	**Observed Rate Constant k_{obs}, (min^{-1})**	**Empirical Rate Constant $k_{obs}/\alpha(HFeO_4^-)$, (min^{-1})**	
SMX	0.114±0.024	*6.910±1.454*	0.074±0.008	*7.982±0.885*	*7.2*
TMP	0.052±0.008	*3.141±0.479*	0.035±0.003	*3.759±0.321*	*8.2*
NAP	0.124±0.007	*7.482±0.400*	0.084±0.009	*9.048±0.975*	*9.0*
CBZ	0.058±0.011	*3.515±0.676*	0.040±0.003	*4.244±0.326*	*9.4*

Note:
When [Cl^-] = 0 M, pKa_3 = 7.227 $\Rightarrow$ $\alpha(HFeO_4^-)$ = 0.0165 at pH 9.0
When [Cl^-] = 0.1 M, pKa_3 = 6.971 $\Rightarrow$ $\alpha(HFeO_4^-)$ = 0.0092 at pH 9.0
The difference (%) refers to the relative standard deviation between the two mean values of empirical rate constants from without and with the presence of chloride, respectively.

Table S4. Accurate mass measurement of SMX and its oxidation products (OPs) in Fe(VI) only and in Fe(VI)+HCO_3^- systems, respectively.

Comp	RT (min)	Formula $(M+H)^+$	Experimental *m/z*	Calculated *m/z*	Error (ppm)	Proposed Structure	Fe(VI) only	Fe(VI) + HCO_3^-
SMX	4.510	$C_{10}H_{11}N_3O_3S$	254.05936	254.05994	-2.28	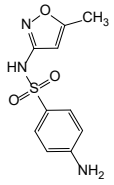	√	√
OP-98	1.756	$C_4H_6N_2O$	99.05592	99.05584	0.81	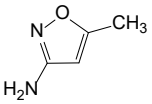	√	√
OP-123	4.257	$C_6H_5NO_2$	124.03960	124.03985	-2.02	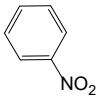	√	√
OP-267	4.632	$C_{10}H_9N_3O_4S$	268.03870	268.03920	-1.87	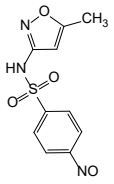	√	√
OP-269	4.397	$C_{10}H_{11}N_3O_4S$	270.05466	270.05485	-0.70	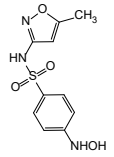	√	√
OP-283	4.885	$C_{10}H_9N_3O_5S$	284.03387	284.03412	-0.88	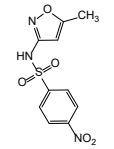	√	√

OP-285	4.431	$C_{10}H_{11}N_3O_5S$	286.04907	286.04977	-2.45	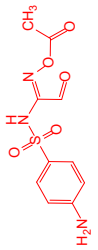	×	√
OP-299	4.842	$C_{10}H_9N_3O_6S$	300.02844	300.02903	-1.97	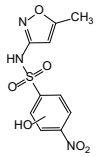	√	√

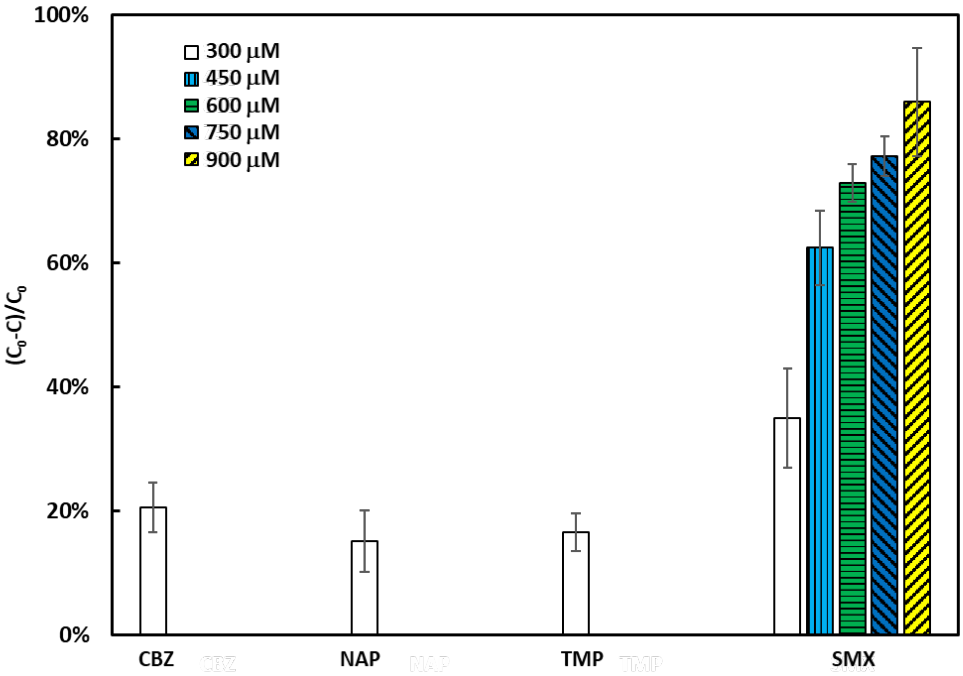

Figure S1. Effect of Fe(VI) dosage on the removal of pharmaceuticals in synthetic hydrolyzed urine (SHU). Initially, [pharmaceutical] = 10.0 µM, [Fe(VI)] = 300.0-900.0 µM, pH = 9.0, T = 25.0 °C, reaction time < 1 min, and n = 2

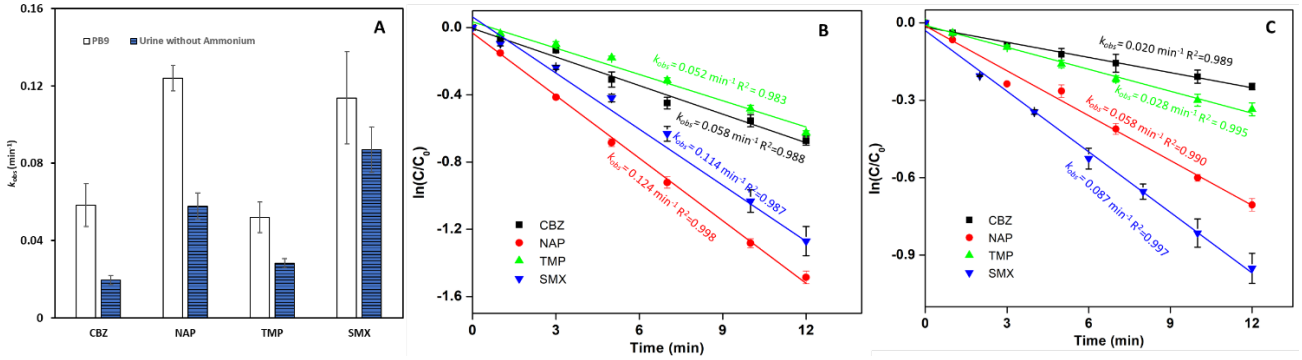

Figure S2. Effect of urine matrix (without ammonium) on Fe(VI) oxidation of pharmaceuticals (A); The kinetics of Fe(VI) oxidation of pharmaceuticals in PB9 (B) and in hydrolyzed urine without ammonium (C). Initially, [Pharmaceutical] = 10.0 μM, [Fe(VI)] = 300.0 μM, pH = 9.0, T = 25.0 °C, n = 2 for CBZ, NAP and TMP, n = 3 for SMX.

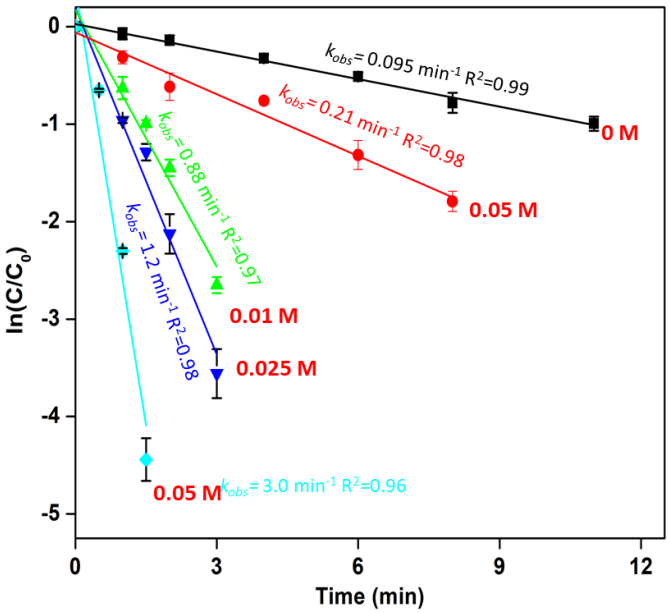

Figure S3. Effect of ammonium on degradation of SMX in 10.0 mM phosphate bufferInitially, [SMX] = 10.0 μM, [Fe(VI)] = 300.0 μM, [ammonium]= 0 - 0.5 M, pH = 9.0, T = 25.0 °C, and *n* = 2 Note: "ammonium" is defined as the sum of NH_3 + NH_4^+.

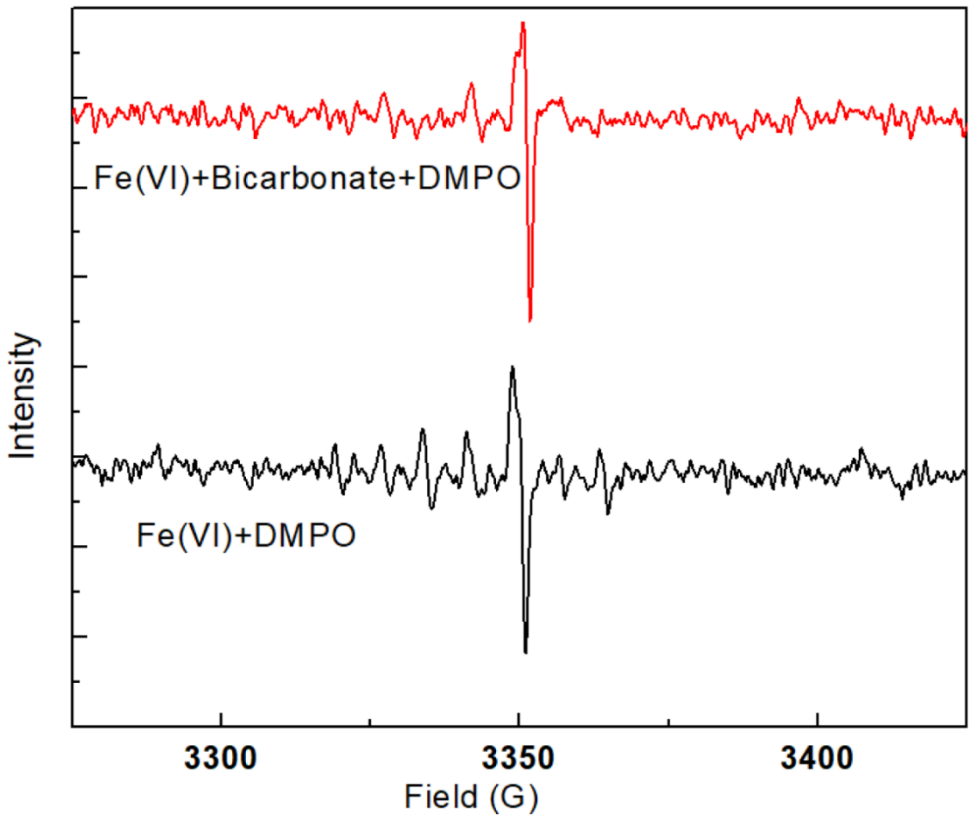

Figure S4. EPR spectra of the reaction solutions by Fe(VI) treatments with or without bicarbonate. Note: No obvious EPR signals were observed. (Experimental conditions: $[Fe(VI)]_0$ = 300.0 μM, $[HCO_3^-]$ = 250.0 mM, $[DMPO]_0$ = 100.0 mM, pH = 9.00 ± 0.05).

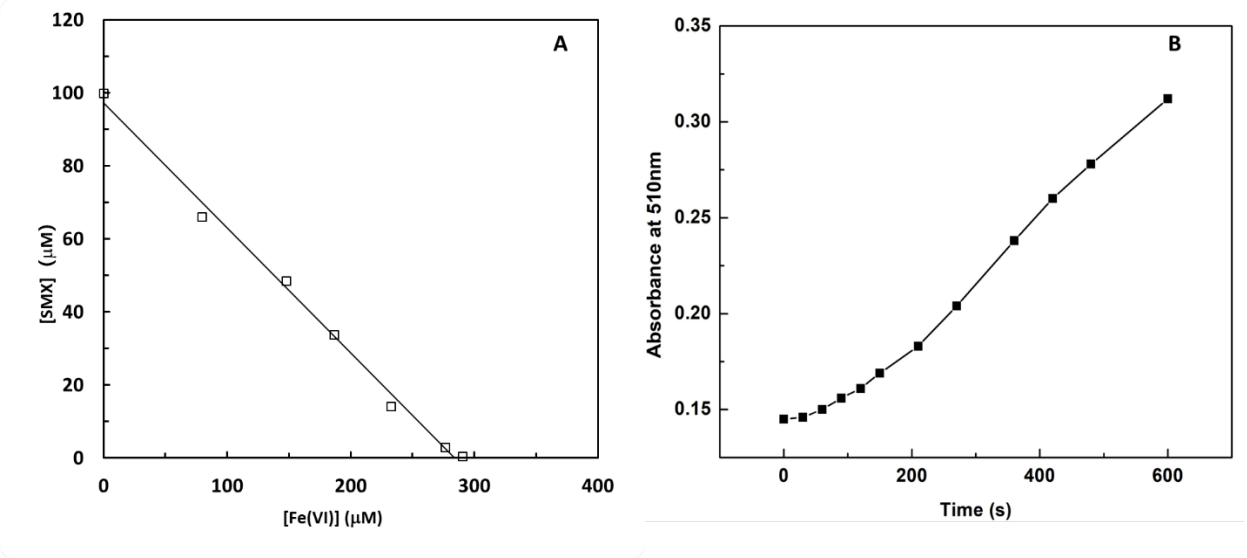

Figure S5. (A) Plot of consumption of SMX in reaction with Fe(VI) in the presence of 0.25 M bicarbonate at pH 9.0. (B) Absorbance-time curve of Fe(VI) oxidation of SMX in the presence of 0.25 M bicarbonate and 4.0 mM 1,10-phenanthroline at pH 9.0; initially, Fe(VI) = 210.0 μM and [SMX] = 10.0 μM.

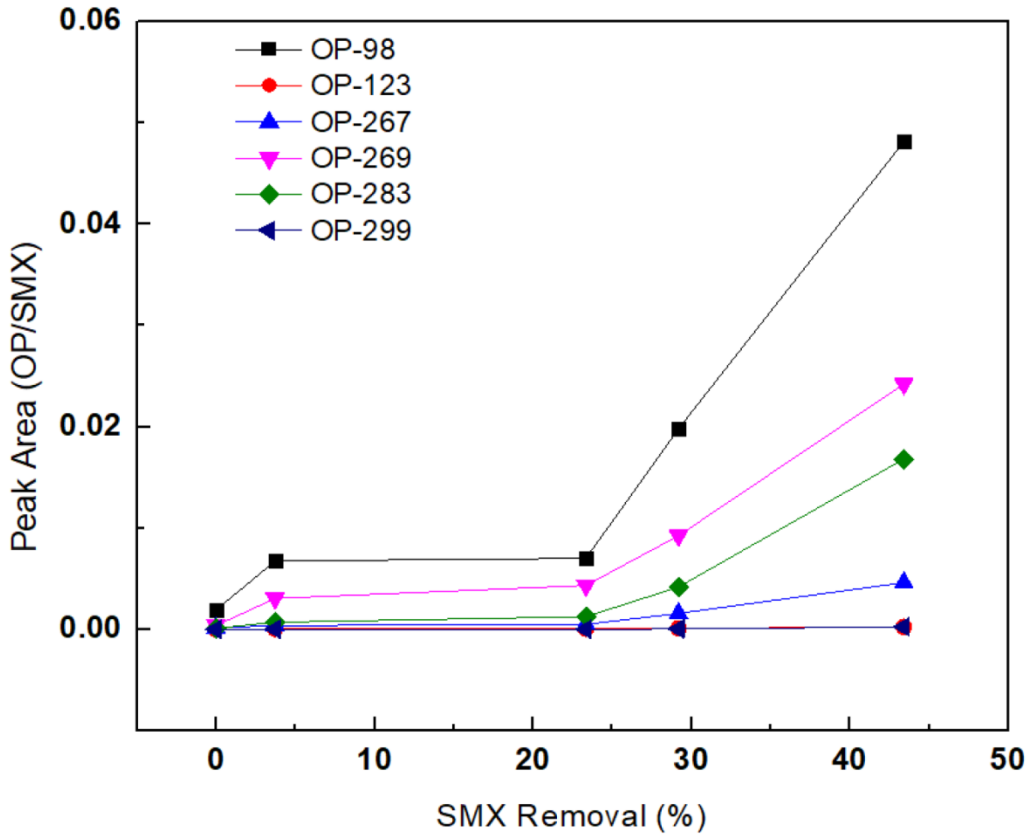

Figure S6. Peak area of SMX products by Fe(VI) in 10.0 mM PB solution at pH 9.0. Peak area of each product was divided by area of the initial parent compound (SMX).

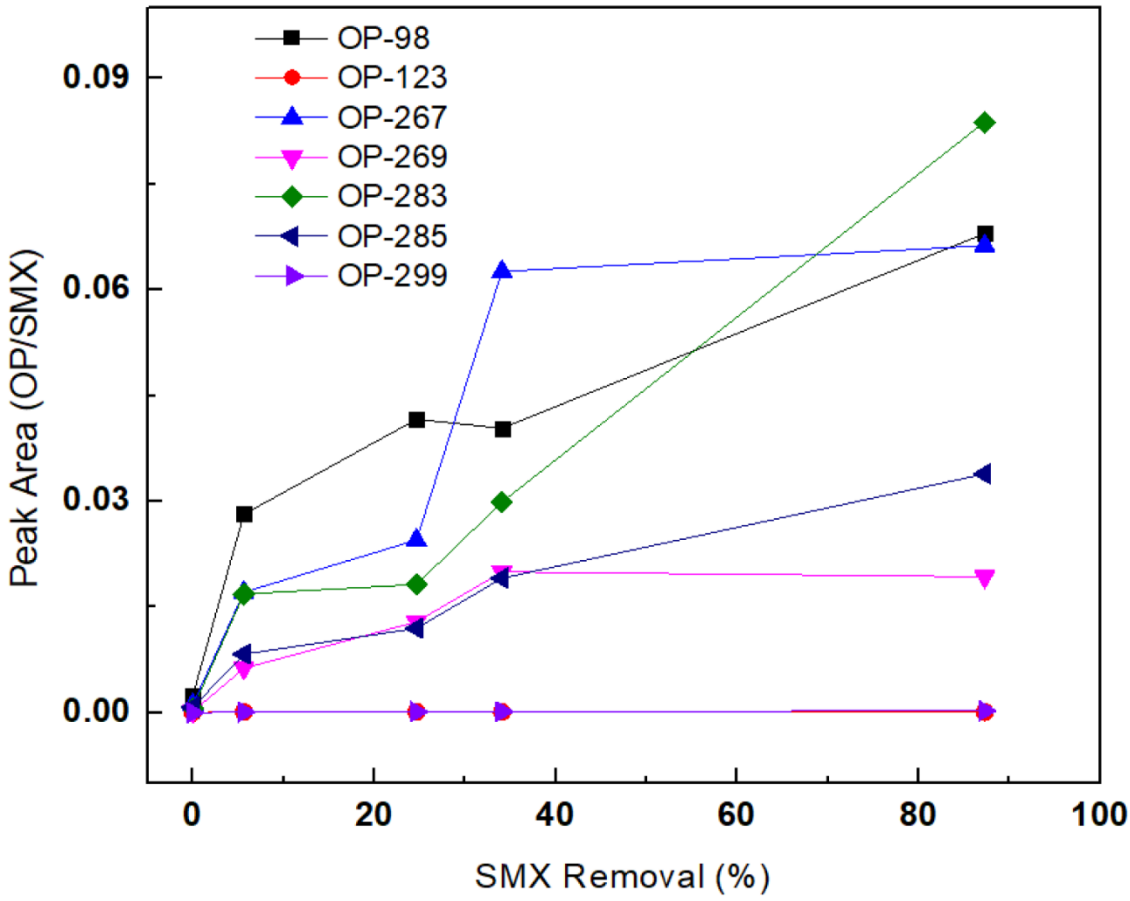

Figure S7. Peak area of SMX products by Fe(VI) in 0.25 M bicarbonate solution at pH 9.0. Peak area of each product was divided by area of the initial parent compound (SMX).

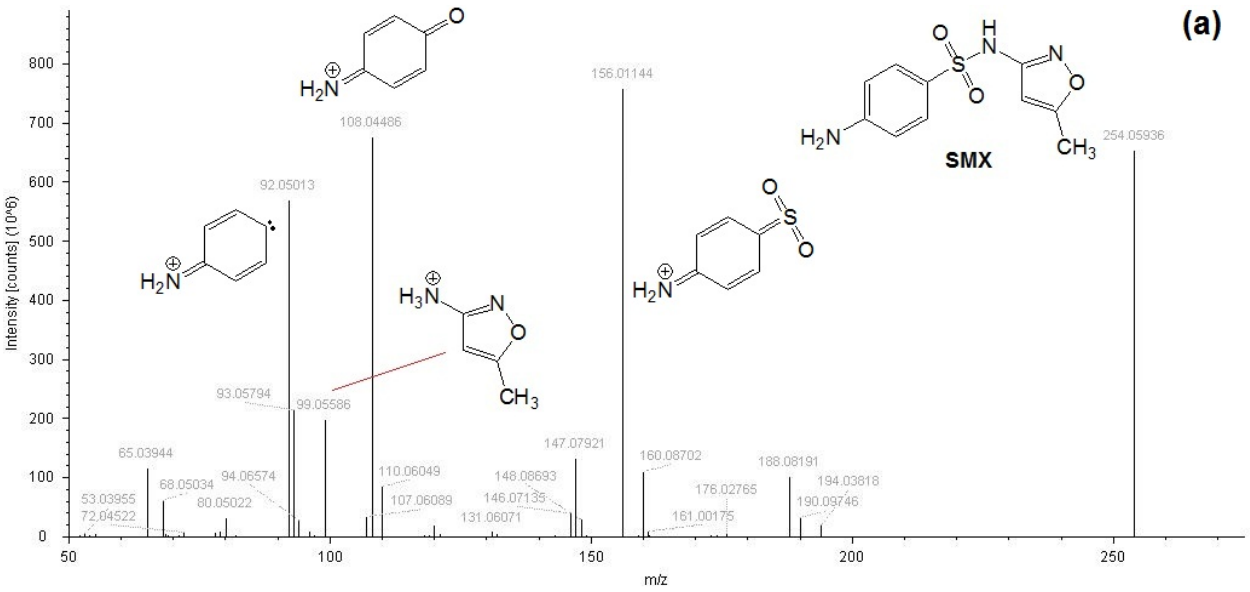
(a)
SMX
Intensity [counts] (10^6)
m/z
156.01144
108.04486
254.05936
92.05013
99.05586
93.05794
147.07921
160.08702
188.08191
65.03944
68.05034
94.06574
110.06049
148.08693
176.02765
194.03818
53.03955
72.04522
80.05022
107.06089
146.07135
131.06071
161.00175
190.09746

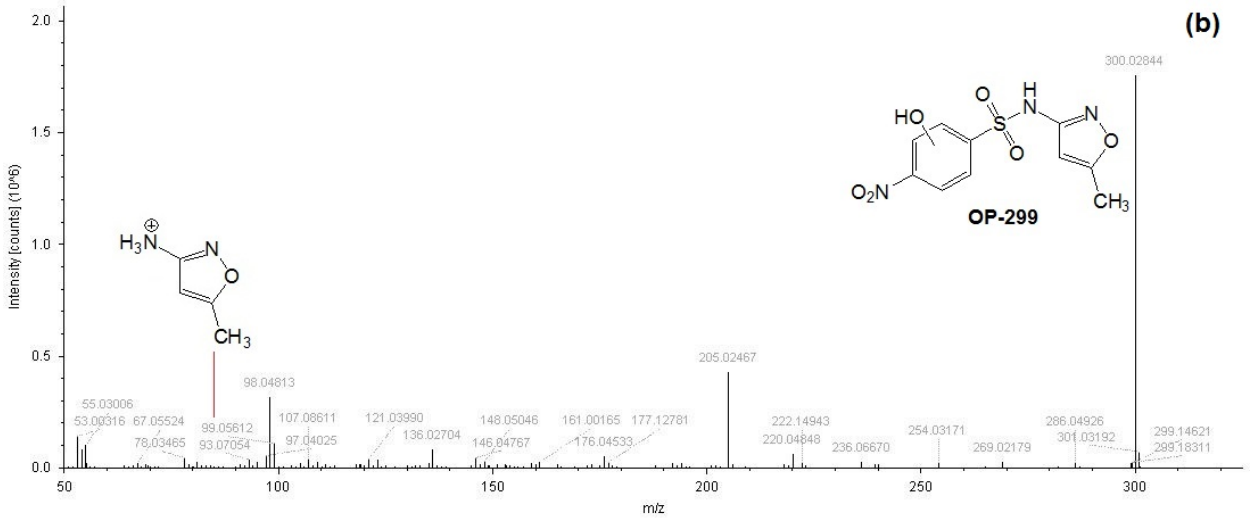
(b)
OP-299
Intensity [counts] (10^6)
m/z
300.02844
205.02467
98.04813
55.03006
53.00316
67.05524
78.03465
99.05612
93.07054
107.08611
97.04025
121.03990
136.02704
148.05046
146.04767
161.00165
176.04533
177.12781
222.14943
220.04848
236.06670
254.03171
269.02179
286.04926
301.03192
299.14621
299.18311

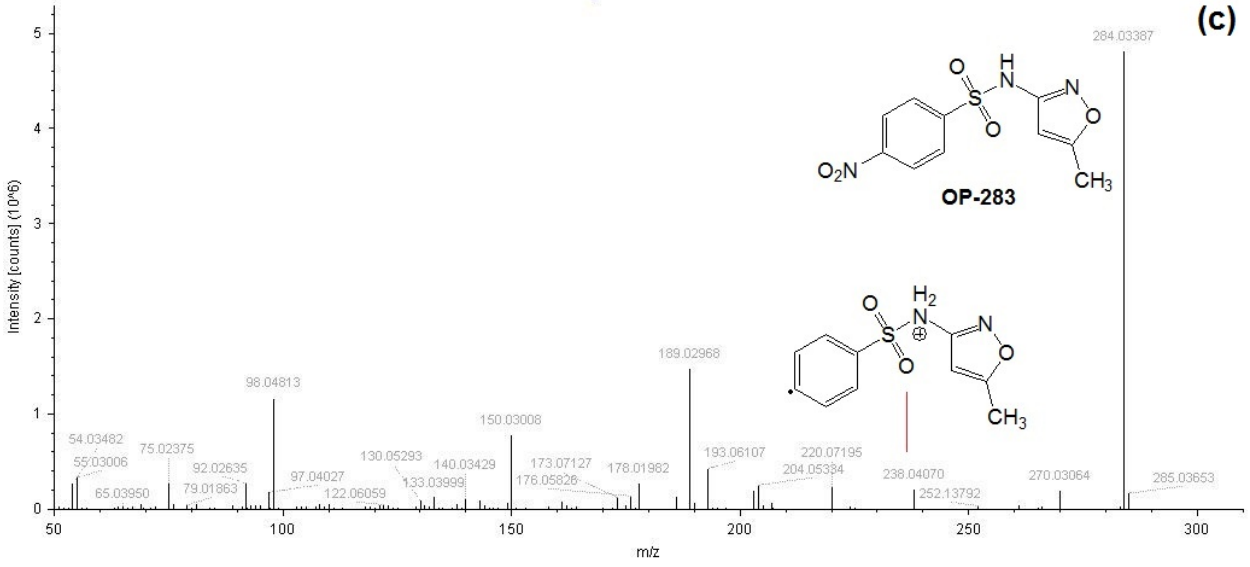
(c)
OP-283
Intensity [counts] (10^6)
m/z
284.03387
189.02968
98.04813
150.03008
54.03482
55.03006
75.02375
92.02635
65.03950
79.01863
97.04027
122.06059
130.05293
133.03999
140.03429
176.05826
173.07127
178.01982
193.06107
220.07195
204.05384
238.04070
252.13792
270.03064
285.03653

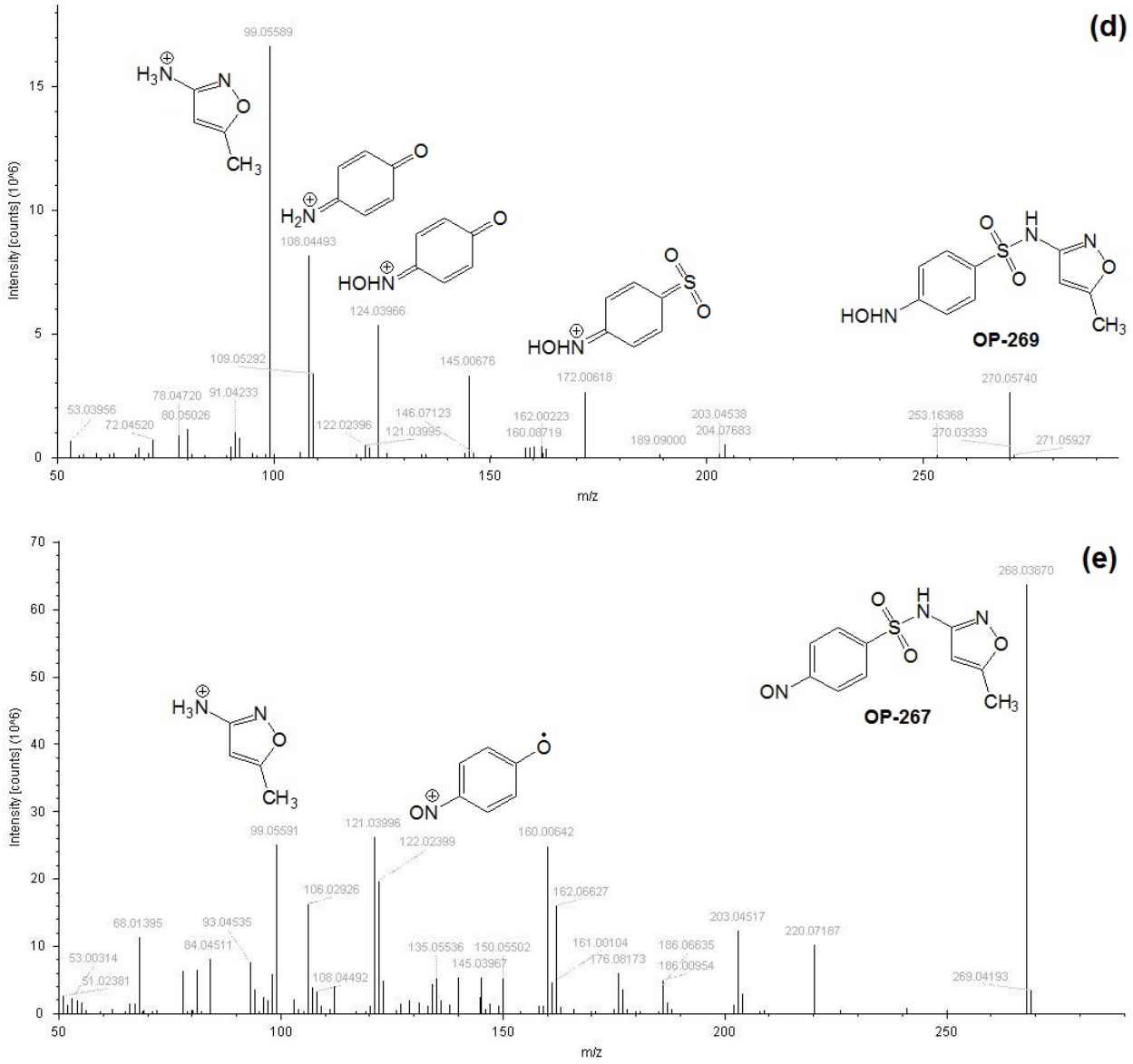

Figure S8. The LC/MS/MS spectra of SMX (a) and its OPs (b, OP-299; c, OP-283; d, OP-269; e, OP-267) with their proposed fragmentation structures.

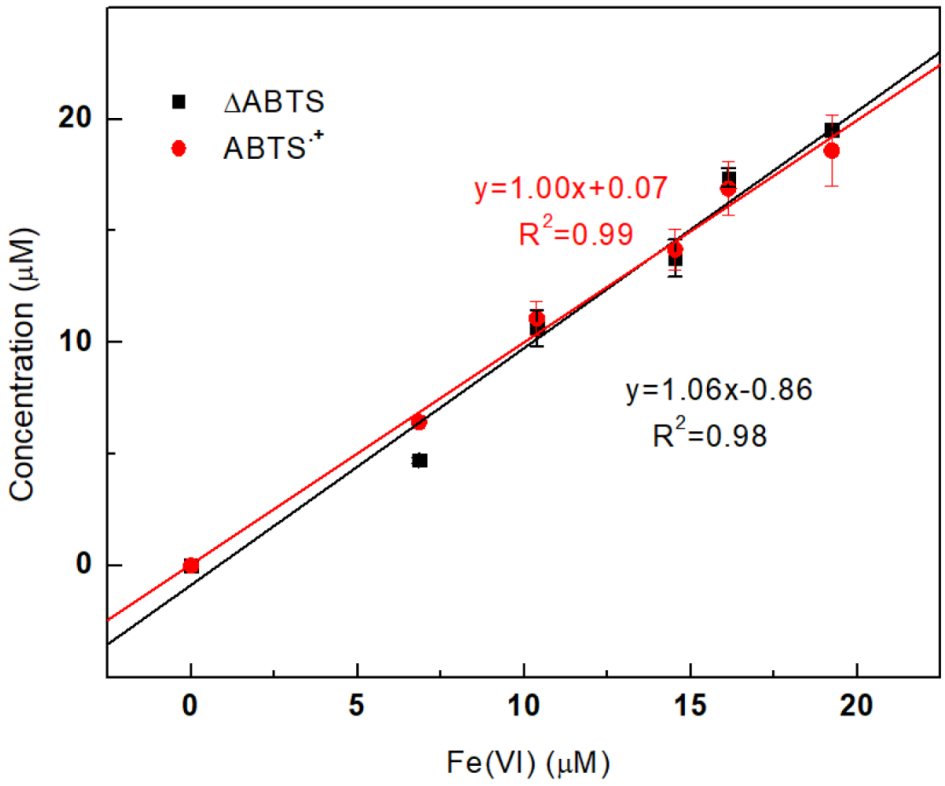

Figure S9. Reaction stoichiometries between Fe(VI), ABTS and $ABTS^{\bullet+}$ in 10.0 mM phosphate buffer at pH 9.0. Initially, $[ABTS]_0$ = 100.0 μM, $[Fe(VI)]_0$ = 0 - 20.0 μM.

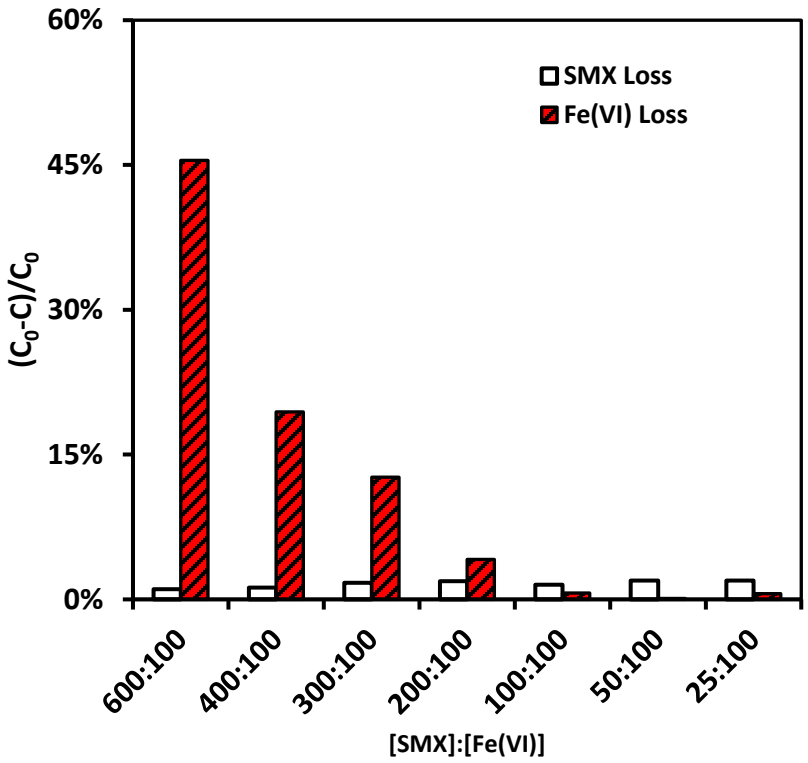

Figure S10. Free Fe(VI) & SMX loss under different [SMX]:[Fe(VI)] ratios within 15 s. [SMX] = 25.0 - 600.0 μM, [Fe(VI)] = 100.0 μM, [PB] = 10.0 mM (pH 9.0).

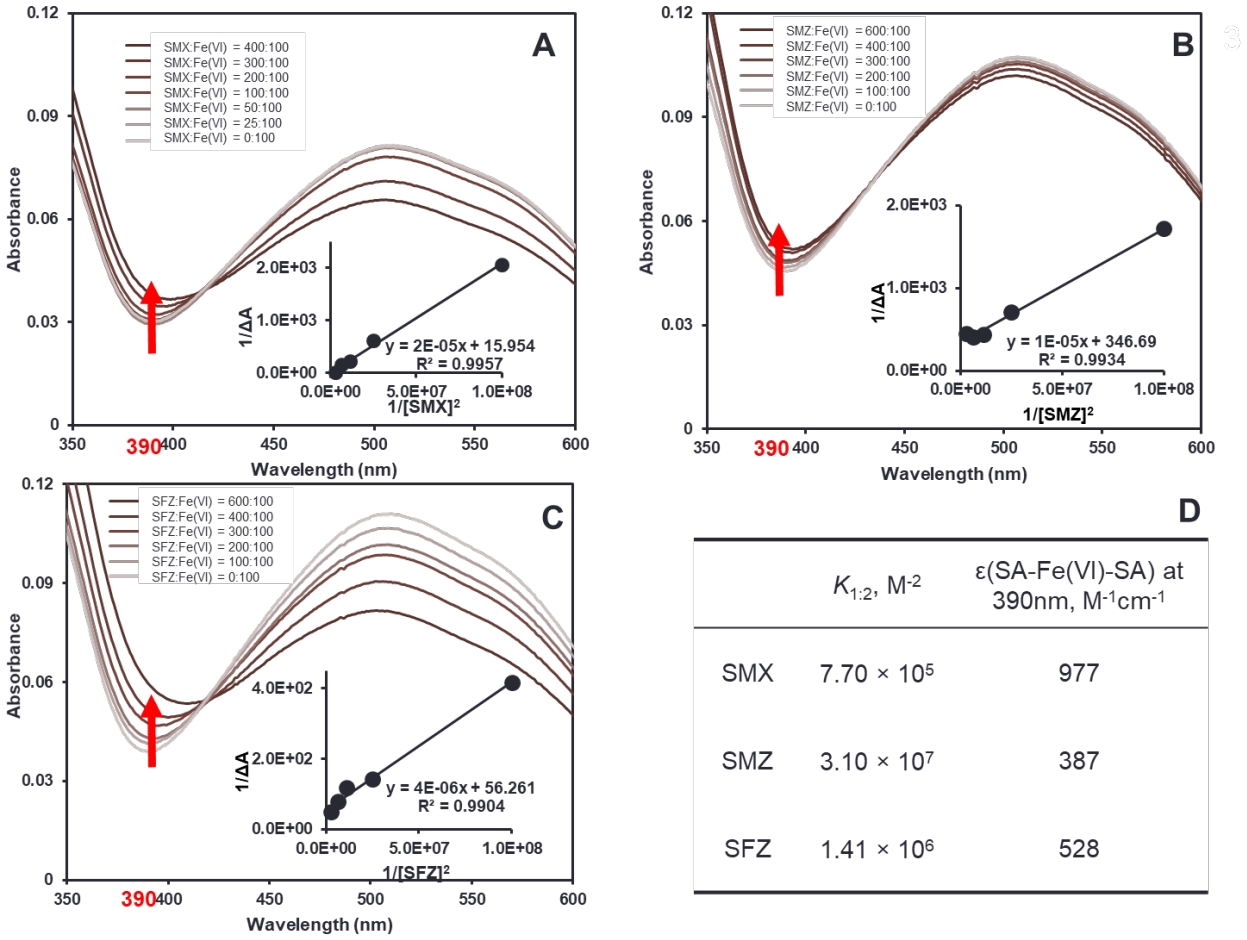

	$K_{1:2}$, M^{-2}	ε(SA-Fe(VI)-SA) at 390nm, $M^{-1}cm^{-1}$
SMX	7.70×10^5	977
SMZ	3.10×10^7	387
SFZ	1.41×10^6	528

Figure S11. UV-vis spectra of SMX (A), SMZ (B) and SFZ (C) complexation with Fe(VI) within 15 s, [SA] = 0 - 600.0 μM, [Fe(VI)] = 100.0 μM, [PB] = 10.0 mM (pH 9.0). Inset: Linear relationship by plotting $1/[SA]^2$ versus $1/\Delta$(Absorbance); (D) The summary of $K_{1:2}$ and absorptivities of different SA-Fe(VI)-SA complexes.

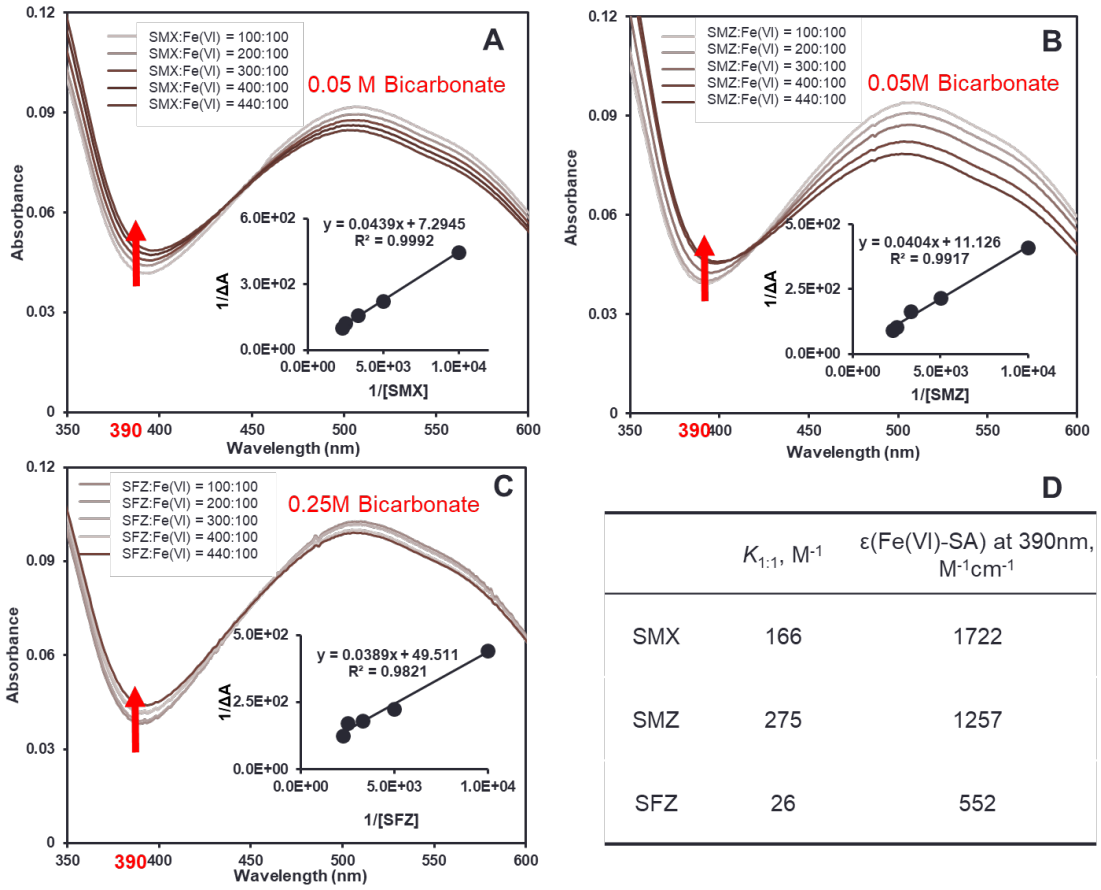

	$K_{1:1}$, M^{-1}	ε(Fe(VI)-SA) at 390nm, $M^{-1}cm^{-1}$
SMX	166	1722
SMZ	275	1257
SFZ	26	552

Figure S12. UV-vis spectra of SMX (A), SMZ (B) and SFZ (C) complexation under different bicarbonate concentrations with Fe(VI) within 15 s, [SA] = 0 - 440.0 μM, [Fe(VI)] = 100.0 μM, [PB] = 10.0 mM (pH 9.0). Inset: Linear relationship by plotting 1/[SA] versus 1/Δ(Absorbance); (D) The summary of $K_{1:1}$ and absorptivities of different Fe(VI)-SA complexes.

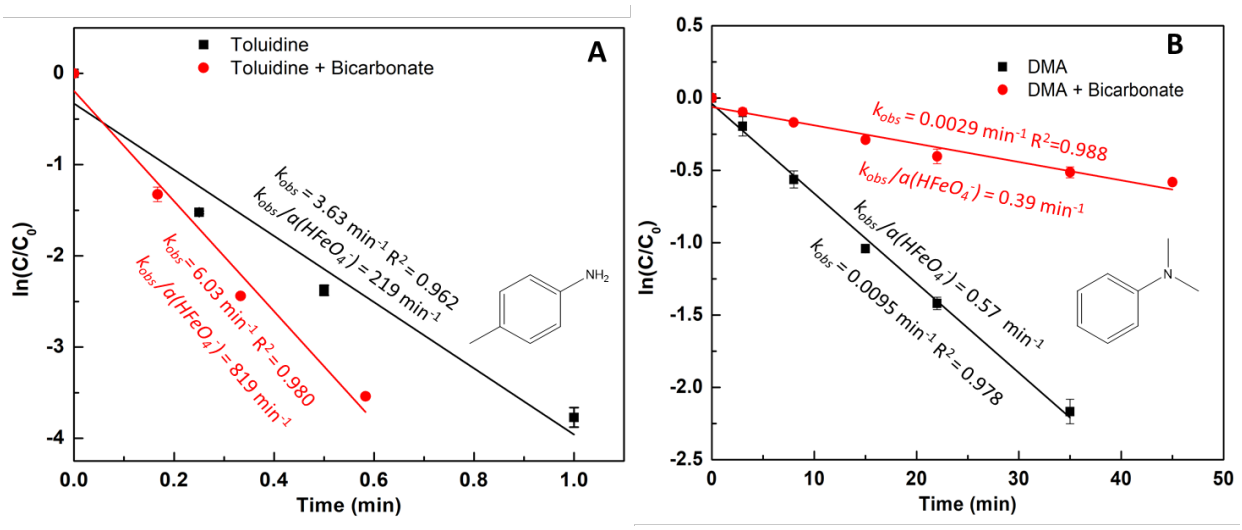

Figure S13. Degradation of *p*-toluidine (**A**) and DMA (**B**) by Fe(VI) with and without bicarbonate. Initially, [Substrate] = 10.0 μM, [Fe(VI)] = 300.0 μM, [HCO_3^-] = 0.25 M, pH = 9.0 (10.0 mM phosphate buffer), T = 25.0 °C, and n = 2.

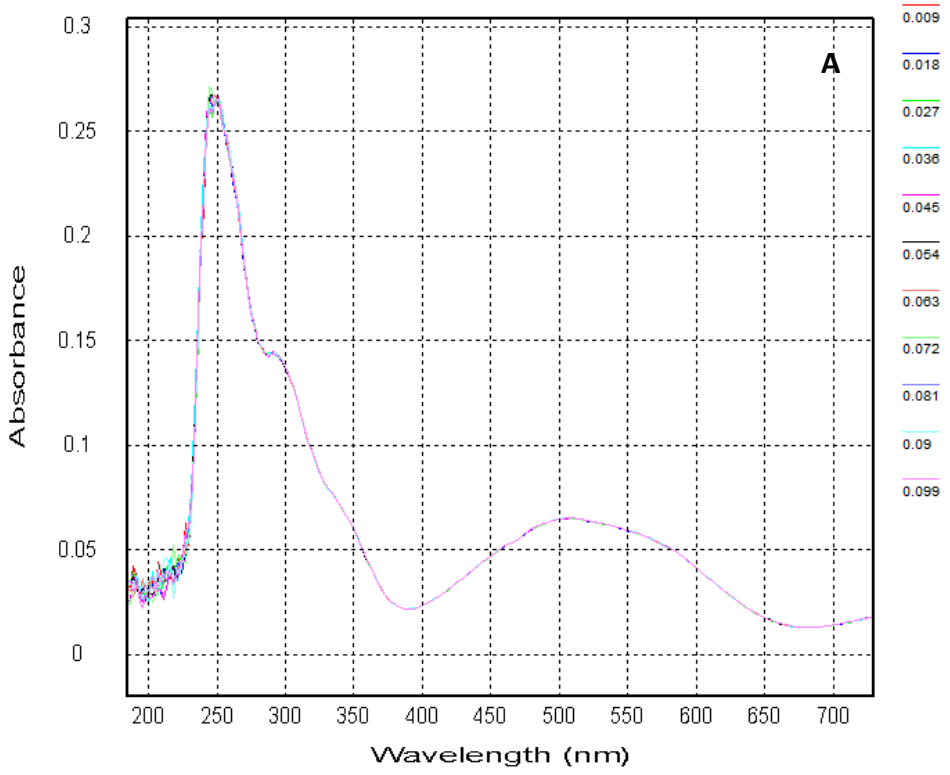
A
Absorbance
Wavelength (nm)
0.3
0.25
0.2
0.15
0.1
0.05
0
200
250
300
350
400
450
500
550
600
650
700
0.009
0.018
0.027
0.036
0.045
0.054
0.063
0.072
0.081
0.09
0.099

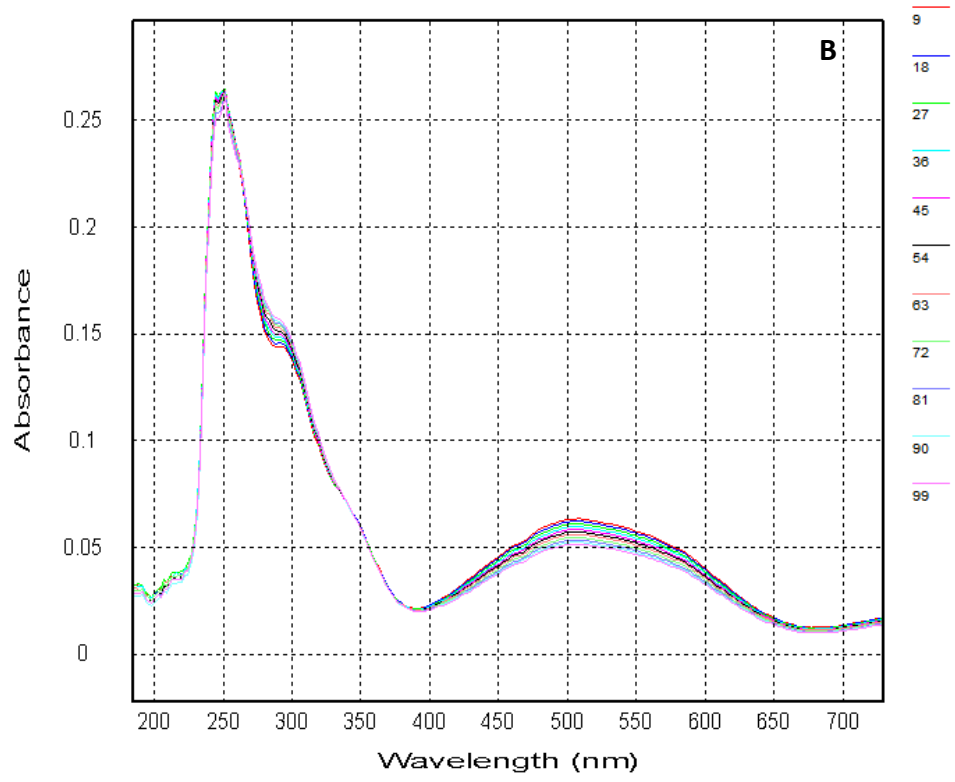
B
Absorbance
Wavelength (nm)
0.25
0.2
0.15
0.1
0.05
0
200
250
300
350
400
450
500
550
600
650
700
9
18
27
36
45
54
63
72
81
90
99

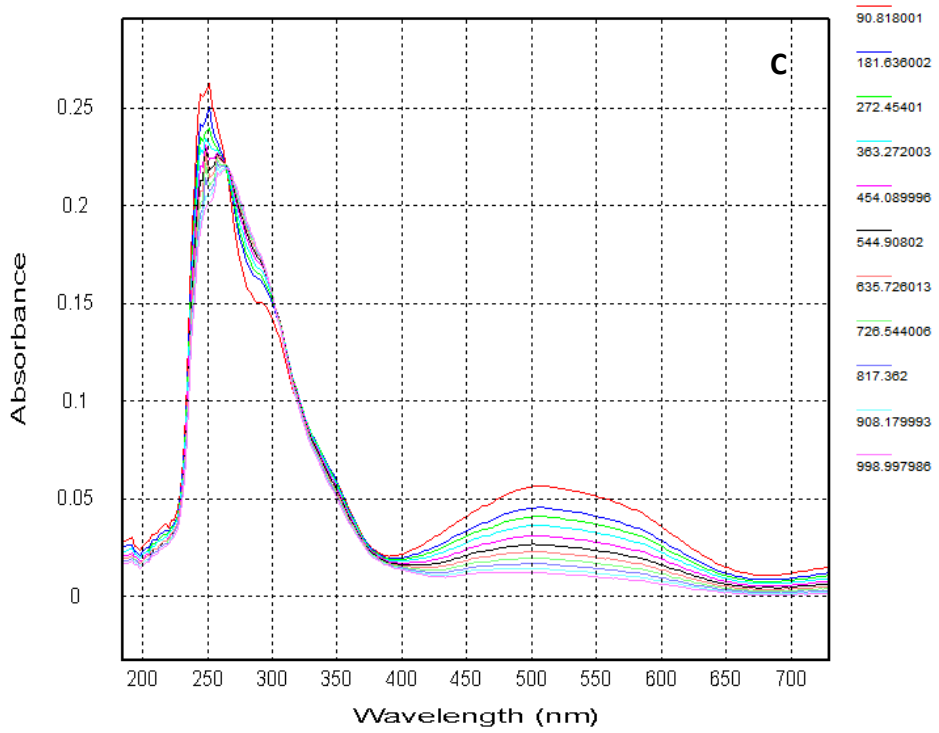

Figure S14. Stopped-flow UV-Vis spectra of Fe(VI) and SMX in the presence of 0.25 M bicarbonate. [Fe(VI)] = 300.0 μM, [SMX] = 10.0 μM, pH = 9.0 (10.0 mM phosphate buffer), reaction time = 0.1 s (A), 100.0 s (B), and 1000.0 s (C).

REFERENCES

(1) He, F.; Zhao, W.; Liang, L.; Gu, B. Photochemical oxidation of dissolved elemental mercury by carbonate radicals in water. *Environ. Sci. Technol. Lett.* **2014**, *1* (12), 499-503.

(2) Lee, Y.; Kissner, R.; von Gunten, U. Reaction of ferrate(VI) with ABTS and self-decay of ferrate (VI): Kinetics and mechanisms. *Environ. Sci. Technol.* **2014**, *48* (9), 5154-5162.

(3) Wang, H.; Yao, H.; Sun, P.; Li, D.; Huang, C.-H. Transformation of tetracycline antibiotics and Fe(II) and Fe(III) species induced by their complexation. *Environ. Sci. Technol.* **2016**, *50* (1), 145-153.

(4) Wen, X.; Tan, F.; Jing, Z.; Liu, Z. Preparation and study the 1:2 inclusion complex of carvedilol with β-cyclodextrin. *J. Pharmaceut. Biomed. Anal.* **2004**, *34* (3), 517-523.

(5) Kolar, M.; Novak, P.; Siskova, K. M.; Machala, L.; Malina, O.; Tucek, J.; Sharma, V. K.; Zboril, R. Impact of inorganic buffering ions on the stability of Fe(VI) in aqueous solution: Role of the carbonate ion. *Phys. Chem. Chem. Phys.* **2016**, *18* (6), 4415-4422.